A PREPRINT

August 5, 2020

Hydrogeologic and Geochemical Distinctions in Salar Freshwater Brine Systems

L. A. Munk[1] 0000-0003-2850-545X, D. F. Boutt[2] 0000-0003-1397-0279, B. J. Moran[2] 0000-0002-9862-6241, S. V. McKnight[2] 0000-0002-6013-193X, J. Jenckes[1] 0000-0002-1811-3076

[1]Department of Geological Sciences, University of Alaska Anchorage

[2]Department of Geosciences, University of Massachusetts Amherst

Corresponding author: Lee Ann Munk (lamunk@alaska.edu)

Key Points:

- Distinct hydrogeologic and geochemical zones are inherent in salar freshwater-brine systems.
- Lagoons in the Transition Zone are perched by complex subsurface geology, depend on inflow waters and respond to climate over time.
- Transition zone brines are geochemically distinct from nucleus brines and are hosted by more diverse aquifer geology.

Abstract

The Salar de Atacama contains one of the world's most important lithium resources and hosts unique and fragile desert ecosystems. Water use issues of the hyper-arid region have placed it at the center of global attention. This investigation is the first robust assessment of a salar system to incorporate geology, hydrogeology, and geochemistry of the aquifer system in the inflow, transition zone and the nucleus. Multiple physico-chemical parameters including conductivity, temperature, Li and Na, and multiple isotopic indicators (^{3}H, δD, and ^{87}Sr/^{86}Sr) all conclude that the transition zone water zones are distinct and separated from the brine in the halite nucleus. Geochemical modeling indicates that the inflow and transition waters are saturated with respect to calcite whereas lagoons, transition zone margin, halite nucleus margin and nucleus waters are saturated with respect to calcite, gypsum, and halite, and the transition zone brines at depth display a broader range of saturation states as compared to the nucleus brines. Long-term remote-sensing of surface water body extents suggest that extreme precipitation events are the primary driver of surface area changes (by a factor of 2.7 after storm). A major finding from this work is that the subsurface brines in the transition zone and the halite nucleus are geochemically and hydraulically disconnected from the groundwater discharge features (lagoons) over modern time scales which has far reaching implications for understanding the link between brine and freshwater.

Plain Language Summary

Salar systems are of intense global focus because of associated water and resource use issues. The freshwater brine systems that are unique to these areas support both resource development and community needs. Until now, rigorous, data-driven analyses of the hydrologic characteristics of these systems have not been provided. This is the first integrated analysis of freshwater-brine systems that characterize salars. The work includes an analysis of 1) hydrogeochemical pathways of fresh to saline waters including multiple physical, chemical and isotope tracers, 2) aquifer geology and hydraulic properties, 3) geochemical modeling to verify secondary processes contributing to aquifer heterogeneity and the formation and sustainability of lagoons and 4) remotely sensed data for tracking temporal changes in the extent of water bodies. Springs, wetlands, lagoons, and open pools in the transition zone of the Salar de Atacama are controlled by the influx of freshwater from upgradient, the hydraulic properties of the complex

subsurface geology, and climate. Transition zone brines and brines in the halite nucleus are geochemically and hydraulically disconnected from the groundwater discharge features. The methods are transferrable to salar systems on a global scale and can be used by multiple stakeholders for decision making regarding resources and environment.

1 Introduction

The marginal environments of salar systems are unique ecological and hydrogeological regions of great importance in arid to hyper-arid climates (Rosen, 1994; Warren, 2016; Pigati et al., 2014). These distinctive places have become one of the most significant areas of concern in regions where groundwater and/or brine extraction are relied on for human use including resource development and fresh water sources used by communities (Tyler et al., 2006; Houston at al., 2011; Warren, 2010). As demand for water sources continues to increase (Wang et al., 2018; Zipper et al., 2020; Gleeson et al., 2020) it is critical to have a complete and scientifically based assessment of these transitional zone regions where freshwater discharges and evaporates above brackish and brine water in the subsurface. This process is what supports the formation of springs, wetlands or marshes (vegas), and lagoons (lagunas) to form a unique ecosystem that can be found on the margins of all salars on a global scale. However, the extent of development of these groundwater discharge features is unique among each salar which is reflective of the morphology, geology, elevation, and overall hydrology of each basin. The work presented here is the first rigorous and comprehensive geochemical and hydrogeological study of one of the most important transition zones in the world which is that along the southern region of the Salar de Atacama (SdA). However, the methods, conceptual model, and functioning of these systems is translational to all salar systems.

A handful of studies have suggested that it is the pumping of brine that has caused the water table of the SdA to decrease since the early 1980s at the onset of lithium brine production (e.g. Marzuela et al., 2019; Salas et al., 2010), and these observations are also reported in various industry documents and other non-peer-reviewed articles. These studies are flawed because they do not consider or include 1) impacts of long-term climate influence on the water levels, 2) the fact that large volumes of recharge water are sourced outside of the topographic watershed, 3) the specific hydrogeologic heterogeneity of the marginal aquifer system which controls freshwater-brine interaction and 4) field-based ground truth observations to test proposed models as well as ignoring paleohydrological contributions to modern discharge when determining water balance (e.g. Marzuela et al., 2020). Therefore, the previous water balances used to interpret the SdA system must be reconsidered. Previous work by Corenthal et al. (2016) and Munk et al. (2018) indicates that there is an imbalance between modern water and solutes delivered to the salar demonstrating that water in the basin is not sourced only from the immediate watershed but that sources of water from adjacent watersheds to the north, east and south are required to close the water balance. In summary, those works point to three exceptionally important facts about how the salar and marginal salar systems work: 1) additional water and solutes outside the topographic watershed is needed to explain the mass of the voluminous halite deposit, 2) the lagoons that exist on the margin of the salar have persisted for millions of years and have their water sourced primarily from long (old) flow paths as well as pulsed recharge from modern precipitation events, and 3) the lagoons and other freshwater sourced features that are persistent, such as springs, marshes, and lagoons are highly compartmentalized and are disconnected hydrogeologically from the massive halite nucleus (core of the salt flat) and its brine, but they rely on recharge waters from upstream aquifers in the basin.

This paper is focused on a detailed hydrogeochemical investigation of a major lagoon system at SdA which is based on a rigorously sampled flow path of the shallow groundwater system and important surface water bodies (Figures 1 and 2). A new conceptual model of the zones of the upper fresh/brackish regime and the lower brine regime are developed based on the hydrogeochemistry, subsurface geology, and hydraulic properties. Munk et al. (2018) defined that 21% of the water flux in the entire SdA basin discharges to the southern transition zone and lagoon systems. The entire basin contributes 3.11 m^3/s to all of the lagoon systems in SdA including the south and east lagoons (Munk et al., 2018). The Punta Brava Lagoon Complex (PBLC) is representative of 0.51 m^3/s (GW2 and GW3 from Munk et al., 2018) out of the 4.81 m^3/s of total recharge in the basin and the Salada-Saladita-Interna (SSI) lagoon system fed by the southeast inflow is representative of 0.48 m^3/s (SW/GW1, SW/GW2, GW4 from Munk et al., 2018) making these lagoon systems of particular interest. The work presented here also builds on the Li brine ore deposit model developed in Munk et al., (2016 and 2018) which indicates that the Li brine in the nucleus of SdA originated from water-rock interaction removing Li from high Li host rocks (ignimbrite with up to ~2000 ppm Li) in the basin which is subsequently concentrated by evaporation and ultimately by fractional crystallization of halite. Here we add a detailed investigation describing how the transition zones and their water features are decoupled hydrogeologically from the halite nucleus. This has far reaching implications for both environmental and resource issues surrounding these important Li resources on a global scale.

2 Geologic and Hydrogeologic Setting of the Salar and Transition Zone

2.1 Regional Salar de Atacama Geology and Hydrogeology

The SdA is a significant topographic depression located within the volcanic arc of the Central Andes of Chile (Reutter et al, 2006). The salt flat (salar) at the basin floor covers 3,000km^2 at an elevation of 2,300m and is closed to the north, south and east by the Andean Cordillera (>5,500 m) and the Cordillera de Domeyko (>3,500 m) to the west. The rim of high volcanic peaks to the east and southeast delineates the SdA topographic watershed, encompassing over 17,000 km^2, and the western margin of the Altiplano-Puna Plateau (Allmendinger et al., 1997; Jordan et al, 2010). This vast, internally drained plateau ranging in elevation from 4,000 m to 6,000 m is underlain by the Altiplano-Puna Volcanic Complex (APVC) (Silva, 1989; Silva, 1989a); a succession of volcanic units deposited over the last 10 Ma by caldera forming eruptions which produced over 15,000 km^3 of dense-rock equivalent ignimbrites, small volume mafic centers and numerous stratovolcanoes (Strecker et al., 2007; Ward et al., 2014). The volcanic complex and eastern slope of the basin is primarily composed of andesitic, rhyolitic, dacitic and some basaltic volcanic rocks with alluvial, fluvial and aeolian sediments and sedimentary rocks of primarily re-worked volcanic material (Schmitt, 2001; WMC, 2007). The stratovolcanoes including the high peaks on the topographic divide and possibly those buried under younger volcanic deposits are generally of high permeability (Gardeweg & Ramirez, 1987; WMC, 2007). The regionally extensive, voluminous ignimbrites are characterized by a remarkably homogenous composition that is predominantly calcalkaline dacite (Schmitt, 2001; Ward et al., 2014).

Miocene ignimbrite units draped across the region and alluvial fans along the flanks of the SdA basin appear to be important for transporting fluid to the springs emerging from the slopes and margins of the salar (Jordan et al., 2002; Mather & Hartley, 2005). The thick ignimbrite sequences and other volcanic rocks that occur within the SdA and blanket the surrounding high elevation areas, specifically the modern units (<5 Ma) are characterized by welded and unwelded layers of varying thicknesses and extent (Houston & Hart, 2004). The unwelded ignimbrite sheets have high infiltration capacity and permeability, and they likely constitute the major flow paths of local and regional groundwater, while welded ignimbrites and other sequences of low hydraulic conductivity may act as important confining units (Houston, 2009; Herrera et al., 2016). Large accumulations of sedimentary and conglomerate sequences and buried alluvial fans such as those near the topographic divide could provide conduits for deep groundwater transport to the eastern slope (Wilson & Guan, 2004; Houston, 2009). Vertical leakage through fractured volcanic material and across stratigraphy may constitute flow paths with longer residence times.

The southeastern slope of SdA south of the Tumisa volcano is bounded to the southwest by the Monturaqui–Negrillar–Tilopozo (MNT) trough, a 60 km long N–S oriented depression and the Miscanti Fault and fold to the east separates the basin from the Andes and controls the development of the intra-arc lakes Miñiques and Miscanti (Rissmann et al., 2015; Aron et al., 2008). A large lithospheric block of Paleozoic rock, bounded by the N-S trending Toloncha fault and fold system and Peine fault is interposed in the center of the southeastern slope forming a major hydrogeologic feature that likely diverts groundwater as well as generally restricting groundwater flow through this zone (Breitkreuz, 1995; Jordan et al., 2002; Reutter et al., 2006; Gonzalez et al., 2009; Boutt et al., 2018). The fold and thrust belt architecture of the basin slope is manifested in several thrust fault systems of varying depths and length but which generally trend N-S, parallel to the SdA salar margin; these faults are thought to be major conduits for groundwater flow to the surface as evidenced by the spring complexes emerging along or in the immediate vicinity of these fault zones (Aron et al., 2008; Jordan et al., 2002). Another important fold and thrust feature is the Tilocalar Peninsula which juts out into the middle of the southern transition zone as well as monoclinal folded ignimbrites to the south. At the salar scale, faults in the subsurface may act as conduits or barriers to fluid (brine) movement.

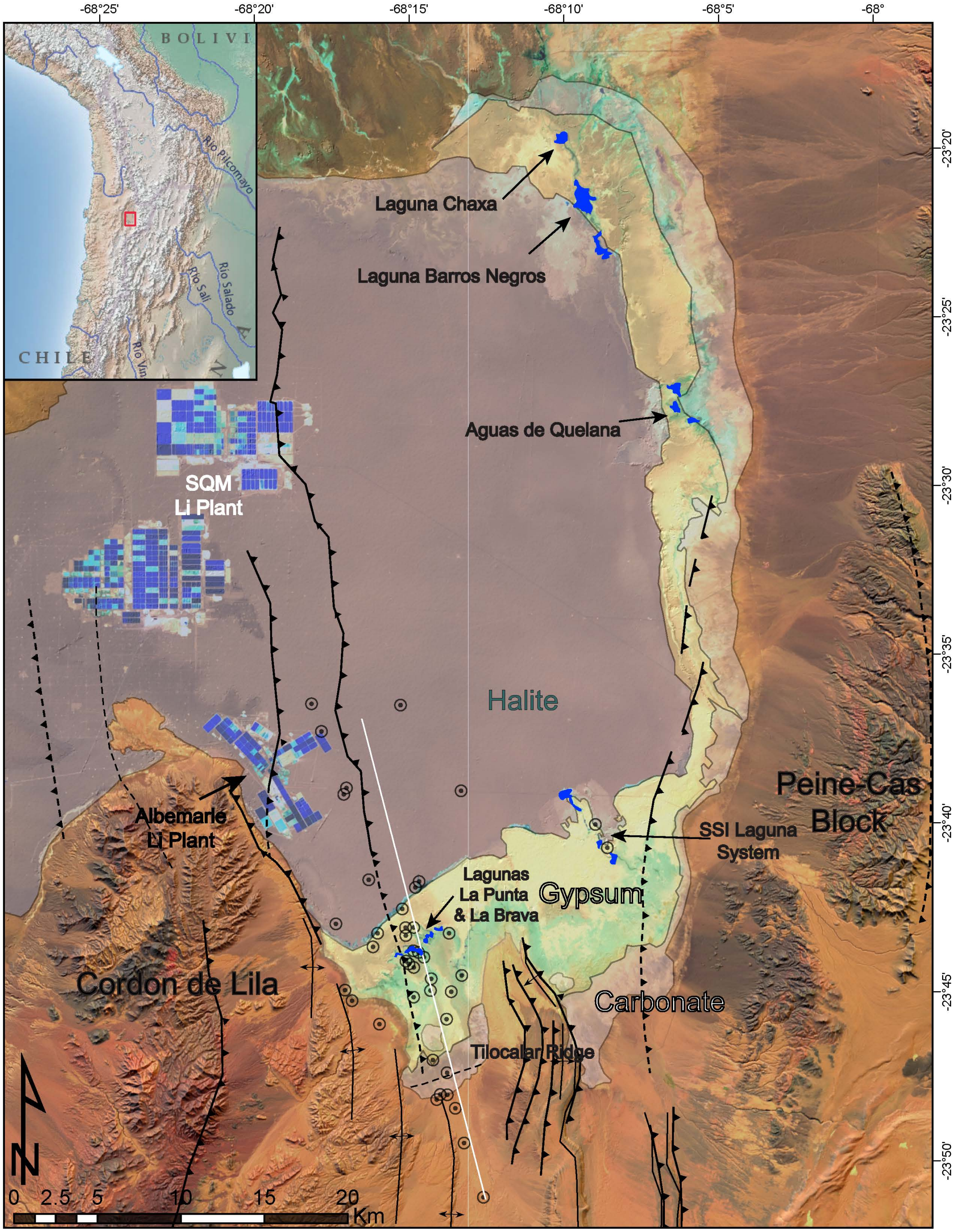

Figure 1. Landsat image of the Salar de Atacama with surface mapped salt crust zones shaded and outlined (carbonate, gypsum and halite) and major lagoon systems identified. These include the Punta Brava Lagoon Complex (PBLC), Salada-Saladita-Interna (SSI) lagoon system, Aguas de Quelana lagoon system, and the Chaxa and Barros Negros lagoon systems. The major faults of the region are also identified and sampling loacations with data reported in this study are shown as black dots.

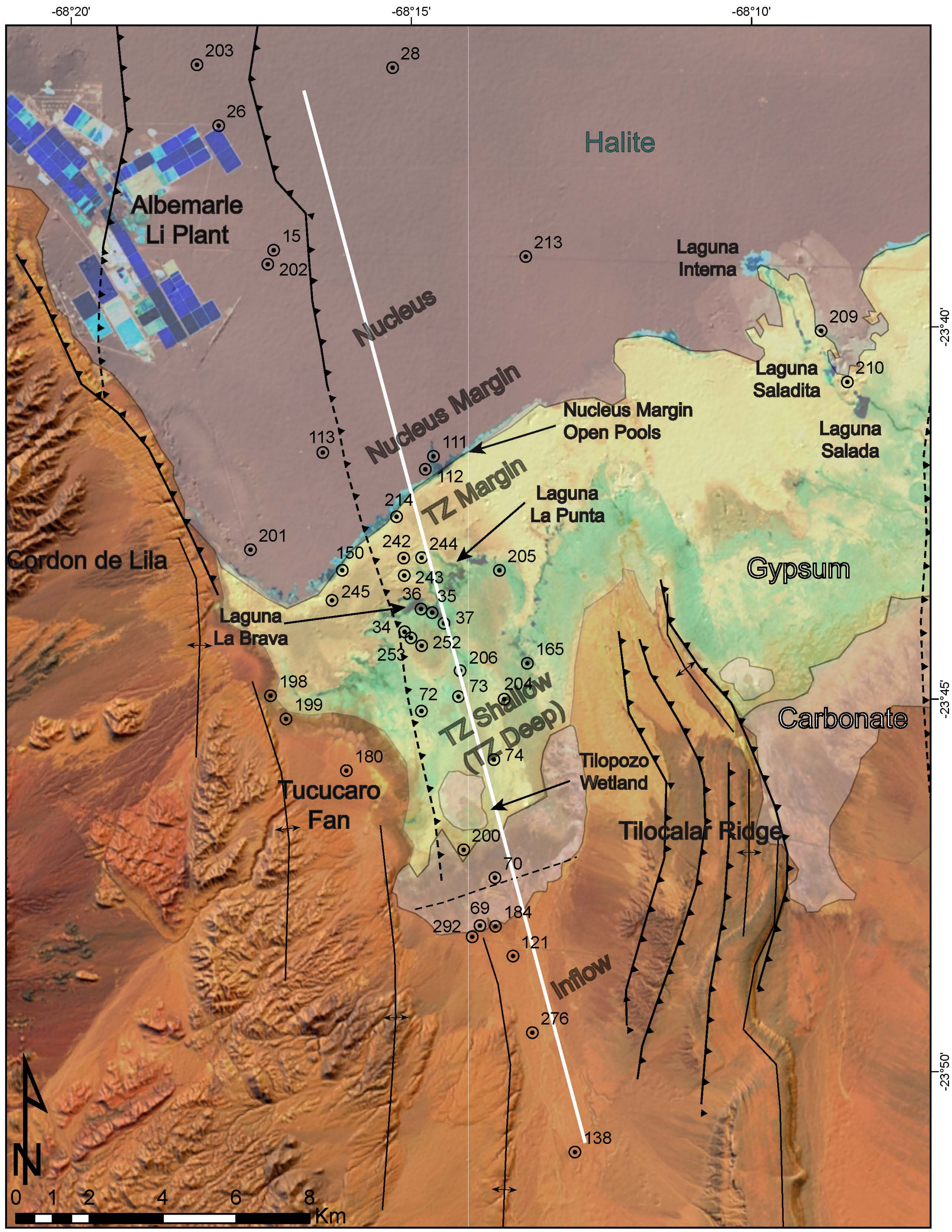

Figure 2. Detailed Landsat image of the southern SdA with surface mapped salt crust zones shaded and outlined as in Figure 1. (carbonate, gypsum, and halite), major lagoon systems, wetlands and the open pools identified. The detailed hydrogeochemical transect is shown as a white line along the upgradient inflow zone through and across the transition zone, to the transition zone and nucleus margins and into the halite nucleus (inflow, TZ = transitions zone shallow and deep, lagoons, TZ margin, nucleus edge and nucleus, also refer to Movie S1 for a virtual field trip across these zones).

2.2 Geology and Hydrogeology of Transition Zones

The transitional zones of salars are known to be composed of a combination of alternating sequences of evaporite deposits (ie. carbonate, gypsum, and halite), minor clastic material (clay, silt, sand, and gravel), and in many cases volcanic ash and ignimbrite deposits. In the SdA basin these geologic units make up the Vilama Formation, the stratigraphy of which is detailed in Lin et al. (2016). The Vilama Formation is up to 1 km thick in places and thickens from the salar margin towards the basin. Figure 1 depicts the distribution of the salt crusts in the marginal transition zones of SdA including the lagoon systems. Although this paper will focus on the details of a hydrogeochemical transect in the south of the basin (Figure 2) primarily because of the robust data set collected in this region, we will also briefly explore the east transition zone and the lagoons located there (Figure 1). Lagoon systems may have subtle differences in the specific hydrogeologic setting with respect to how large the diffuse groundwater regions are that transition to focused inflow. The overall morphology and the extent of flooding surfaces of the lagoons may vary, but similar processes described in this paper apply to other lagoon systems. The SdA marginal transition zone highlights the variability in lagoon morphology as well as the regions between the lagoons and the nucleus margin. For example, the north Chaxa and Barros Negros lagoon systems on the northeast transition zone appear to be fed by a large diffuse groundwater region that becomes channelized into a small stream that feeds three lagoons which are connected by small channels. Undoubtedly this lagoon system also receives inflow from the eastern alluvial fans as small marshes and springs are observed to the east of these lagoons. In some locations there are distinct spherical dissolution features that can be seen within the lagoons, these likely represent regions where there is focused groundwater discharge from longer flow paths that up well into the marginal transition zone region. Further to the south the Aguas de Quelana lagoon system is composed of a series of elongated north-south trending lagoons that occur to the west and down gradient of the massive alluvial fans associated with the very large Tumisa stratovolcano.

Important to understanding the functioning of the transition zone and lagoon systems is the fact that they are underlain by complex heterogeneous subsurface geology that is inherent in the evaporite deposits (Warren, 2006) and interbedded ignimbrites, ashes, and clastic material which together form the aquifer system. There are two main types of carbonate in the marginal zones of the SdA which lie beneath the lagoons along with gypsum and minor halite. One type of carbonate is that which is spatially most common near the edges of the basin where groundwater has discharged in the past and/or in the modern, these carbonates are typically interbedded with alluvial fan deposits and tend to have a vuggy or porous texture characteristic of tufa (Figure 3). The other type of carbonate is the carbonate mud that forms in the lagoons associated with or without microbialite and/or stromatolite deposits. These carbonate deposits can also be observed forming in the modern environment (Sancho-Tomas et al., 2018) and are preserved in multiple sediment cores extracted from the transition zone, these tend to be finely laminated and may have gypsum crystals intergrown or in separate laminae/layers. In the subsurface these deposits occur as lense shaped bodies which are consistent with the general morphology of the modern lagoons and deposits forming today (Figure 3 and Movie S1).

The gypsum deposits observed in core are characterized by either aggregates of prismatic crystals usually with an upward growth pattern or lenticular aggregates which may represent bottom-grown beds where gypsum crystals nucleate in evaporating brine. These textures are found in the upper 10s of meters but at depths below that the texture is finer as gypsum mud or compacted gypsum crystals. We define these textures generally at the meter scale as fine, medium or course and conceptually illustrate this in Figure 3. Small open bodies of water not larger than 10 m in diameter and 1-2 m deep that occur in the transition zone margin are at saturation with respect to gypsum and are characterized by euhedral pyramidal aggregates of gypsum crystals or rosette aggregates that form mounds on the sides and bottom of the pools (these can also be observed in Movie S1 in the region salarward of the lagoons). Gypsum crystals have also been observed to be forming at the surface of these features, these crystals presumably accumulate in layers in these pools over time. Gypsum also occurs as secondary crystals infilling voids as large euhedral crystals or as smaller crystals along fracture surfaces in the ignimbrite. In the deepest (400 m) cores described from the nucleus there are both recrystallized gypsum and halite beds that are highly compacted. Minor anhydrite has been identified in sediment cores as elongate nodules or as thin beds.

Halite in the transition zone occurs either as thin layers up to 10s of cm of primary milky chevron texture deposits that are compacted or secondary infilling of voids of transparent cement in voids or other evaporite, clastic or volcanic deposits. Closer to the transition zone margin and nucleus edge, pinnacle halite and secondary halite with large euhedral crystals up to several cm in diameter are present in the subsurface cores as well as at the surface of the salar. The halite nucleus is characterized by large fractured plates of pinnacle halite at the surface with a reddish color due to the inclusion or trapping of dust particles. In sediment cores from the halite nucleus the pinnacle halite typically occurs in the upper 1 m. Below that secondary or recrystallized halite is very common interspersed with gypsum beds of varying thickness depending on the proximity to the salar margin and even lagoon carbonate deposits can be found in the deeper parts of the nucleus indicating that lagoons were once much further salarward than the present-day position. Volcanic ash and ignimbrite also occur throughout the halite nucleus and act as marker beds that help in stratigraphic correlation (Figure 3) as well as providing geochronologic control. Worth noting is that the vadose zone in the transition zone displays surface deposits of sand-sized lenticular gypsum crystals, chlorides such as halite, and bischofite forming fine-grained crusts within a fracture network of the salt crust.

The hydrostratigraphy of the carbonate, gypsum and halite deposits is variable in the lateral and vertical dimensions and is important for understanding why the inflow water discharges in the locations and the surface distributions observed. The hydraulic conductivity of these materials are summarized in Figure 3.

There are numerous faults located in the south margin of SdA which have been mapped, measured, and inferred by others (ie. Jordan et al. 2007, Martinez et al. 2018, Rubilar et al. 2018) and have been compiled here (Figures 1 and 2) and extrapolated in the conceptual model (Figure 3) based on high resolution seismic and electrical resistivity surveys and where possible ground-truthed with drill cores. Characteristic of the fault zones identified in drill core are zones of fault gouge and breccia that represent damage zones in the area of the faults. We interpret that in at least some areas these faults could act as fluid transport pathways and are responsible to some extent of the movement of recharged water as well as brines (see Figure 3 fault zone conceptualization).

3 Materials and Methods

Water samples used for the PBLC transect analysis were collected for cation, anion, water stable isotopes, Sr isotopes and tritium analyses over the period of 2012-2016. Shallow groundwater samples were obtained from either 4" PVC constructed wells with known screened intervals in the upper fresh to brackish regime generally decimeters below the ground surface and with SC values of up to 60,000 μS/cm and the deeper brine regime with SC values exceeding 200,000 μS/cm. All surface and groundwater samples were collected into clean HDPE bottles after filtering through a 0.45 μm filter. Samples for cation analyses were acidified with high purity concentrated HNO_3. In-situ measurements of temperature, specific conductance, and pH were made at each sampling location at the time of sample collection.

The concentration of major ions and trace elements in the water samples were analyzed using inductively coupled plasma mass spectrometry with a reaction cell for major elements and Li (ICP RC-MS, Agilent 7500c) at the University of Alaska Anchorage. Waters with relatively higher TDS were diluted volumetrically prior to analysis. For ICP RC-MS analysis, samples were acidified to 1% HNO_3 v/v prior to analysis. Quantification was performed using seven external calibration standards ranging from 0.1 to 100 ppb. Drift correction was achieved by online addition of 10 ppb of a four element internal standard mix (Li(7), Y, Ce, and Bi). Calibration verification standards and blanks were run every 10th analysis. Element analysis was verified with external NIST standard SRM 1643d. Samples that exceeded the calibration by 120% were diluted and reanalyzed.

Water samples were analyzed for δ^2H and $\delta^{18}O$ using a Picarro L-1102i WS-CRDS analyzer (Picarro, Sunnyvale, CA) in the ENRI Stable Isotope Laboratory at the University of Alaska Anchorage. International reference standards (IAEA, Vienna, Austria) were used to calibrate the instrument to the VSMOW-VSLAP scale and working standards (USGS45 : δ^2H= -10.3 ‰, $\delta^{18}O$= -2.24 ‰ and USGS46 : δ^2H= -235.8 ‰, $\delta^{18}O$= -29.8 ‰) were used with each analytical run to correct for instrumental drift. Long-term mean and standard deviation records of a purified water laboratory internal QA/QC standard (δ^2H= -149.80 ‰, $\delta^{18}O$= -19.68 ‰) yield an instrumental precision of 0.93 ‰ for δ^2H and 0.08 ‰ for $\delta^{18}O$.

Strontium concentrations and the $^{87}Sr/^{86}Sr$ ratio were measured at the University of Utah Strontium Isotope Geochemistry Laboratory following methods described by Chesson et al.

(2012). During the course of analysis measurements of the isotopic standard SRM 987 yielded a value of 0.710301 ± 0.000007 (1σ, n=51).

Other geochemical data used in this paper originated from an internal industry report. These data generally represent quarterly sampling over a period of up to a decade and are used primarily in establishing seasonal variability and for modeling saturation indices for each hydrogeochemical zone. All data used in this paper can be accessed at (https://doi.org/10.7275/qr40-z439). Modeling results are contained in the supporting document for this paper in Table S1. Insitu measurements of temperature, pH, and SC are reported as well as major and trace element concentrations and anion concentrations. Methods of analysis for major elements are by ICP-OES, trace elements by ICP-MS and anion concentrations by IC, bicarbonate was measured by titration in the laboratory. SGS and ALS commercial geochemical laboratories were utilized for these analyses.

Thirty-meter resolution imagery was downloaded and processed via the LandsatLook Viewer (USGS) for Landsat 7 (1999–present) and Landsat 8 OLI (2013–present). Four images at quarterly increments from years 2003–2016 were analyzed for water coverage extent if possible (January, April, July, October) during the middle of each respective month. If a satellite image during the intended date is unavailable, the next available date is used. All images were imported into ArcGIS and projected to the World Geodetic System 1984 UTM, Zone 19 and overlain on the 30m resolution Land/Water Boundary Time Series (1990–2010) (ESRI). Polygons of the area of lagoons and transitional pools were manually digitized using the Land/Water Time Series base map as a quality control parameter. These features were lumped and associated into their respective groupings. Presence/absence of water is evaluated using qualitative assessment of pixel color. Polygon surface areas are then calculated in square meters. A second interpreter digitized ~3% of the images processed and the calculated differences in areas were within 5% of each other on average. Nucleus margin changes were assessed using LandSat data by digitizing the dark nucleus margin position against the lighter colored modern salt crust. Comparisons are made to legacy geologic maps such as Moraga et al., 1969. Meterological data (see site locations on figure 1) were obtained from Chilean Dirección General de Aguas (DGA). Mean daily and monthly precipitation data for these stations are downloaded from the DGA (http://snia.dga.cl/BNAConsultas/reportes).

4 Results

4.1 Physical and Geochemical Evolution of Inflow, Transition and Nucleus Waters

In order to have appropriate geologic and hydrogeologic context for interpretation of the geochemical properties of each water type in the inflow, transition zone and nucleus system of a salar a detailed understanding of the subsurface is required. Figure 3 is a 3D conceptual model of a section through the inflow zone to the halite nucleus. This model is an integrated conceptualization of all of the water zones, flow paths, subsurface geology (including major faults), hydrogeologic property variability and heterogeneity. It represents the synthesis of detailed (1 m scale) core logging to identify lithologies, observations of secondary mineral occurrence and primary and secondary porosity, correlations of mapped surface and subsurface geology, and hydrogeologic observations and measurements. The result is a comprehensive framework to interpret both hydrogeologic and geochemical processes.

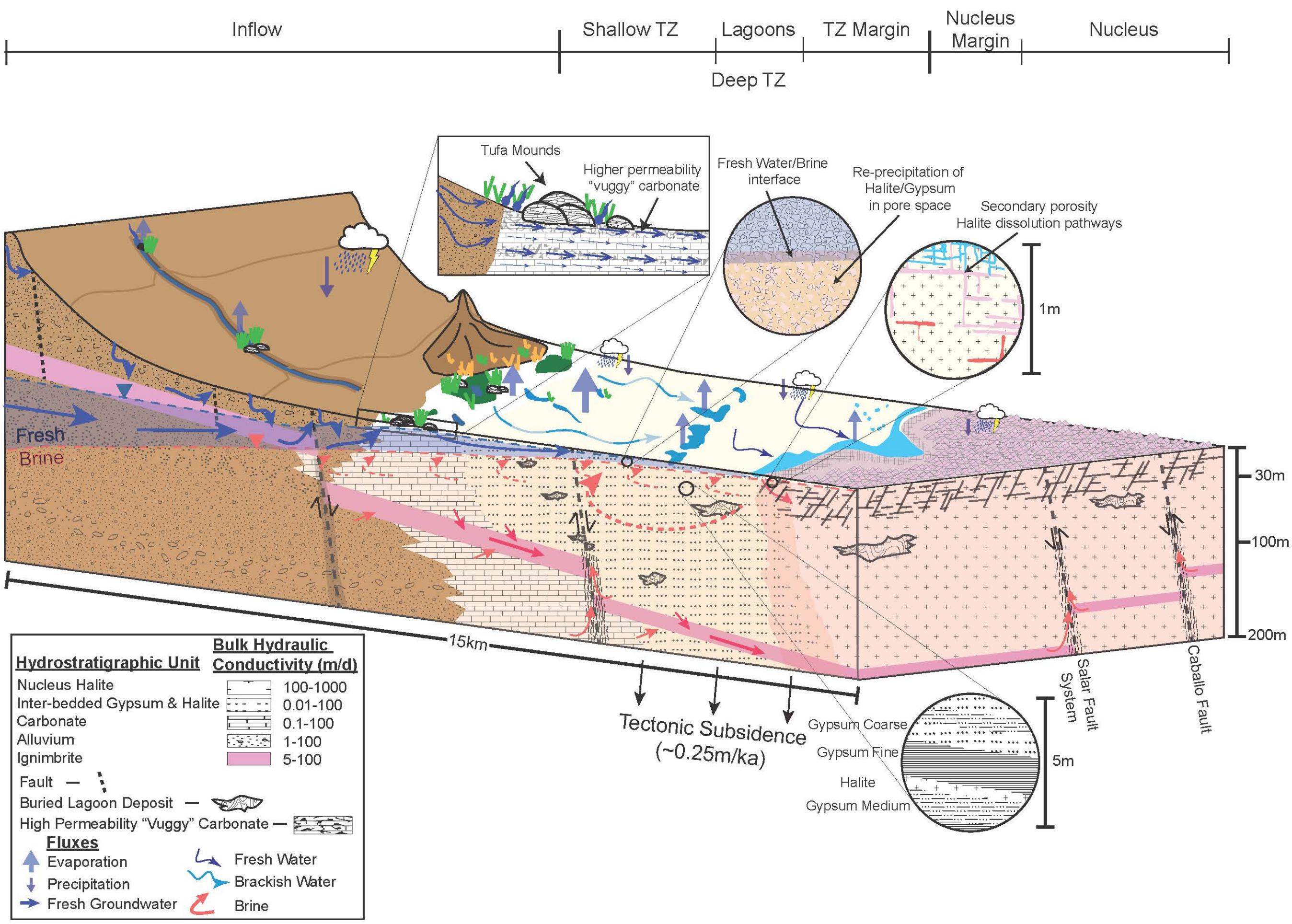

Figure 3. Three-dimensional conceptual diagram of the SdA inflow, transition zone and nucleus water system. Subsurface geology, hydrogeologic flow paths, and groundwater discharge features including the wetlands, springs, lagoons and open pools are depicted. Finer scale characteristics such the heterogeneity in the transition zone geology, primary and secondary porosity and permeability features in the transition zone carbonate, gypsum and halite and halite nucleus are detailed in the circular insets. Important to note are the flow path arrows that depict diffuse groundwater movement in the shallow parts of the transition zone that ultimately end in the lagoons. Wider blue arrows indicate the relative amounts of infiltration (downward) and evaporation (upward). Our virtual field trip across the surface of these water zones is in Movie S1.

Figure 4 illustrates the along flow path (inflow to discharge) variation in multiple physical and geochemical parameters and constituents of shallow groundwater, the PBLC, open pools and the halite nucleus. For reference we use the location of the lagoons as the 0 km point and measure the locations of all the sampling points relative to that up gradient and down gradient (Figure 2). Average concentrations are used to construct these transects in order to capture natural variability as there are changes in some of these values on a seasonal and event (precipitation) basis. The objective is to indicate the general evolution of the water along the 30 km flow path and the distinctions between water compartments in the marginal transition zone and the edge of the halite nucleus which are depicted in 3D view in Figure 3. Generally, the groundwaters in and around the lagoons show significant spatial variability but have much less seasonality than the lagoon waters themselves because they are sustained from inflow waters derived from the MNT aquifer to the south and not as responsive to evaporation as the open water bodies.

The shallow groundwater inflows which are those located about 15 km up gradient of the lagoon discharge point and are the most southern inflow waters we had access to sample are characteristic of the shallow groundwater system which have SC values less than 5,000 µS/cm, high temperatures, highly negative $\delta D\text{-}H_2O_{VSMOW}$ signatures, ^3H values near zero, low Li and Na concentrations (<10 mg/L and <1000 mg/L respectively) and the least radiogenic $^{87}Sr/^{86}Sr$ signatures. However, the $^{87}Sr/^{86}Sr$ show some variability indicating that there could be some mixing of water sources within the south inflow region, and/or this could be representative of the shallow groundwater transitioning from the alluvial fan material aquifer into the ignimbrite aquifer which could impart a more radiogenic signature during water-rock interaction. The $^{87}Sr/^{86}Sr$ values from ignimbrites in the region for the Atana and Toconao ignimbrite pumices range from 0.7106-0.7131 (Lindsay et al., 2001). The waters in the transition zone, the lagoons and nucleus maintain the higher $^{87}Sr/^{86}Sr$ signature. Munk et al. (2018) determined that the sources of water from the south part of the SdA basin and the brines found at elevation all have a very similar $^{87}Sr/^{86}Sr$ signature as the brines in the south part of the halite nucleus.

Between the shallow groundwater inflow zone (shaded blue) and the lagoons (shaded purple) there is an intermediate region of the transition zone where shallow groundwater is impacted by evaporation thereby increasing the SC by an order of magnitude, lowering the temperature by more than 10 ºC, increasing the $\delta D\text{-}H_2O_{VSMOW}$ signature, and increasing both Li and Na concentrations by up to an order of magnitude. From here the water flows into the lagoons through diffuse and focused discharge where the water is further and more extremely exposed to the effects of evaporation in the open water bodies. This is exemplified by an additional order of magnitude increase in SC, although some of this could also be due to interaction with salts that are precipitating and dissolving in this dynamic system (see section 4.2), evaporation is the main driver of these processes on short and long-time scales. The temperature in the lagoons increases due to direct exposure to solar radiation dependent on time of day and since those are surface water body temperatures they are not included in the area of the lagoons in figure 4. The δD-H_2O_{VSMOW} signatures increase by over 40 per mil in the open lagoon water, this dramatic increase is explained by the high evaporation rates at the salar surface. Tritium also increases in the lagoons because of the impacts of direct precipitation (Boutt et al., 2016) mixing with the evaporated water. Lithium concentrations increase by about 2-3-fold in the lagoons and the Na concentrations increase by another order of magnitude both due to evaporation effects in the open water bodies. Calcium concentrations (not shown) are more variable in the lagoons because of the active precipitation of $CaCO_3$ and $CaSO_4$ which can be observed forming in the lagoons typically influenced by the presence of stromatolites.

The water in the region between the lagoons and the open pools/nucleus edge as compared to the lagoon water is characterized by an order of magnitude drop in SC, lower δD-H_2O_{VSMOW} signature by 20 per mil, generally lower ^3H, Li concentrations 2-3-fold lower and Na concentrations an order of magnitude lower indicating an extreme distinction between this water and the lagoon water. Because this water does not have as large of a modern tritium component (unlike the lagoon waters) and that it is brackish but lower in SC and TDS than the lagoon water it is easiest explained as being a mixture of modern precipitation and shallow regional groundwater. In fact, if the lagoon waters were removed from the transect the intermediate waters between the lagoons and the open pools/halite nucleus edge would appear to be a mixture of these two water types. However, the lagoons exist because of constant shallow groundwater discharge and low permeability geologic units in the subsurface (Figure 3) and are in parallel impacted by high evaporation rates.

The open pool water that accumulates at the edge of the halite nucleus in a 2-3 m deep trench-like feature formed by dissolution of halite by fresh precipitation is another geochemically distinct body of water (Movie S1). This water and its ^3H composition were first highlighted by Boutt et al. (2016) as being dominated by precipitation events due to its large fraction of modern water as calculated from the ^3H content. This water is characterized as brine based on its SC values of 200,000 + μS/cm (the same as the brines in the nucleus), the highest δD-H_2O_{VSMOW} measured in any water along the transect due to going towards complete dryness in the trenches, 401

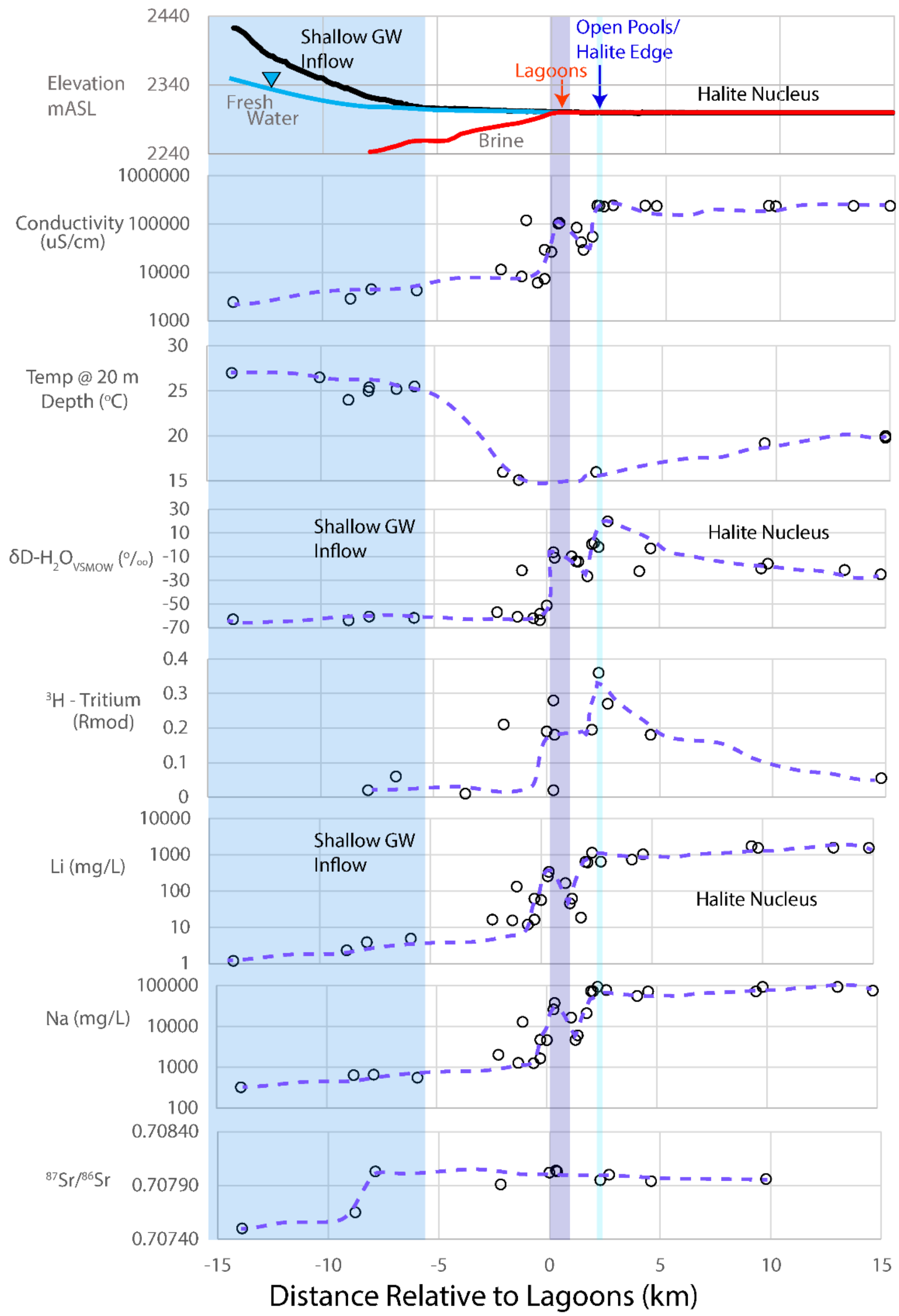

Figure 4. The 30 km hydrogeochemical transect spanning the freshwater-brine salar system (transect location depicted in Figures 1 and 2). The PBLC location is used as the 0 km measuring point for up gradient and downgradient distances. Blue shading denotes the inflow water zone, purple the lagoons, and light blue is the open pools and edge of transition zone margin and halite nucleus. Temperature data for surface water bodies not included due to diurnal variability. Conductivity and ^3H (Rmod) first published in Boutt et al. (2016).

402

the highest ^3H values along the transect indicating that a large percentage of this water is modern precipitation, high Li concentrations on the order of 1000 mg/L and Na concentrations as high as the nucleus brines. These water features are some of the most dynamic in the salar system because they are compartmentalized by the dissolution trench that has formed along the nucleus edge. This water may seep into the nucleus some distance as shown by the signature of of δD-H_2O_{VSMOW} of the open pool water and the decrease in this signature to 5 km distance into the halite nucleus. The nucleus brines have been shown to have enriched δD-H_2O_{VSMOW} signatures along the margin but are generally depleted further salarward (Boutt et al., 2016). The dynamic nature of the open pools and the lagoons is further documented by analysis of satellite images before and after a major rain event at the salar in 2015 in section 3.3 of this paper.

Finally, the nucleus brines are characterized by the highest SC values, intermediate temperatures, intermediate δD-H_2O_{VSMOW} signatures, low to no ^3H, the highest Li and Na concentrations (with the exception of higher Na concentrations in the open pools because of the extreme evaporation that occurs there). In particular the large difference in the δD-H_2O_{VSMOW} signature of the brines as compared to the lagoon water and the fact that there is no ^3H in the brines defines this water as distinct from the lagoon water indicating that there is no connection between the lagoons and the brines in the halite nucleus. Another way to interpret this is that if the nucleus brines and the lagoons were somehow hydrogeologically connected, the geochemistry of the lagoons would be dominated by brine and have a completely different geochemical signature than what is observed and measured.

4.2 Geochemistry of Inflow, Transition Zone and Nucleus Waters

The geochemistry of the waters used in this study aid in defining and classifying the water types of the freshwater-brine system. Guided by the conceptual model in Figure 3 and informed with the general flow path physical and chemical trends in Figure 4 we define seven hydrogeochemical zones in the inflow-transition zone-nucleus system which are 1) inflow, 2) TZ (transition zone) shallow, 3) TZ deep, 4) lagoon, 5) TZ margin, 6) nucleus margin, and 7) nucleus (Figure 5, Movie S1). The major cation and anion, Li and $^{87}Sr/^{86}Sr$ of each zone indicates that the concentrations and ranges of chemical composition and isotopic signatures for inflow and shallow transition zone water are the lowest observed, whereas the lagoon waters are intermediate and the four other zones are composed of higher concentrated brines of varying composition as well as the most radiogenic $^{87}Sr/^{86}Sr$ signatures (Figure 5). Lithium, Na, and K concentrations have similar variability across zones, but are notably on average higher in the nucleus brines compared to the TZ deep brines. Magnesium concentrations have a similar pattern to the alkali metals however, Ca appears to be more variable between the zones, and in particular is lower in the TZ deep brines compared to the nucleus brine and has a larger range in the lagoon waters compared to the other water types. Chloride concentrations are low in the inflow waters, increase in the lagoons with significant variability, are relatively consistent among the TZ margin, nucleus margin and the nucleus waters and somewhat lower with a large range in the TZ deep brines. Sulfate is also lowest in the inflow waters with a general increase in concentration in the lagoons with more variability and is variable among the marginal waters in the TZ and nucleus as well as the nucleus and is lower in the TZ deep brines compared to nucleus brines. Bicarbonate concentrations are the least variable across zones but like most of the geochemical parameters on average lower in the TZ deep brines compared to the nucleus brines, interestingly the inflow waters, lagoons and TZ deep brines all have similar average concentrations. The $^{87}Sr/^{86}Sr$ signatures of the inflow waters and lagoons on average are similar with the inflow waters having the most variability. The marginal waters are also similar but the nucleus brines and TZ brines indicate a more variable and radiogenic signature and the nucleus brines have a less radiogenic signature than the TZ deep brines. This pattern may be attributable to the diversity in aquifer materials for the brines which include the 3.1 Ma Tucucaro ignimbrite. Subsurface diamond drill cores that intercept the ignimbrite in the TZ deep brine region as well as the nucleus show pervasive alteration of the pumice and glassy matrix by interaction with the brine.

In order to further test the processes impacting the water geochemistry along the flow path described in Figure 4 as well as the brines and the marginal waters, equilibrium geochemical modeling was performed on the waters from each of the zones. Vasquez et al. (2013) demonstrated the importance of including geochemical reactions for 2D groundwater flow models for a transect in the northeast part of the SdA. They found that because of the formation of secondary minerals in the shallow subsurface the primary porosity and permeability of the

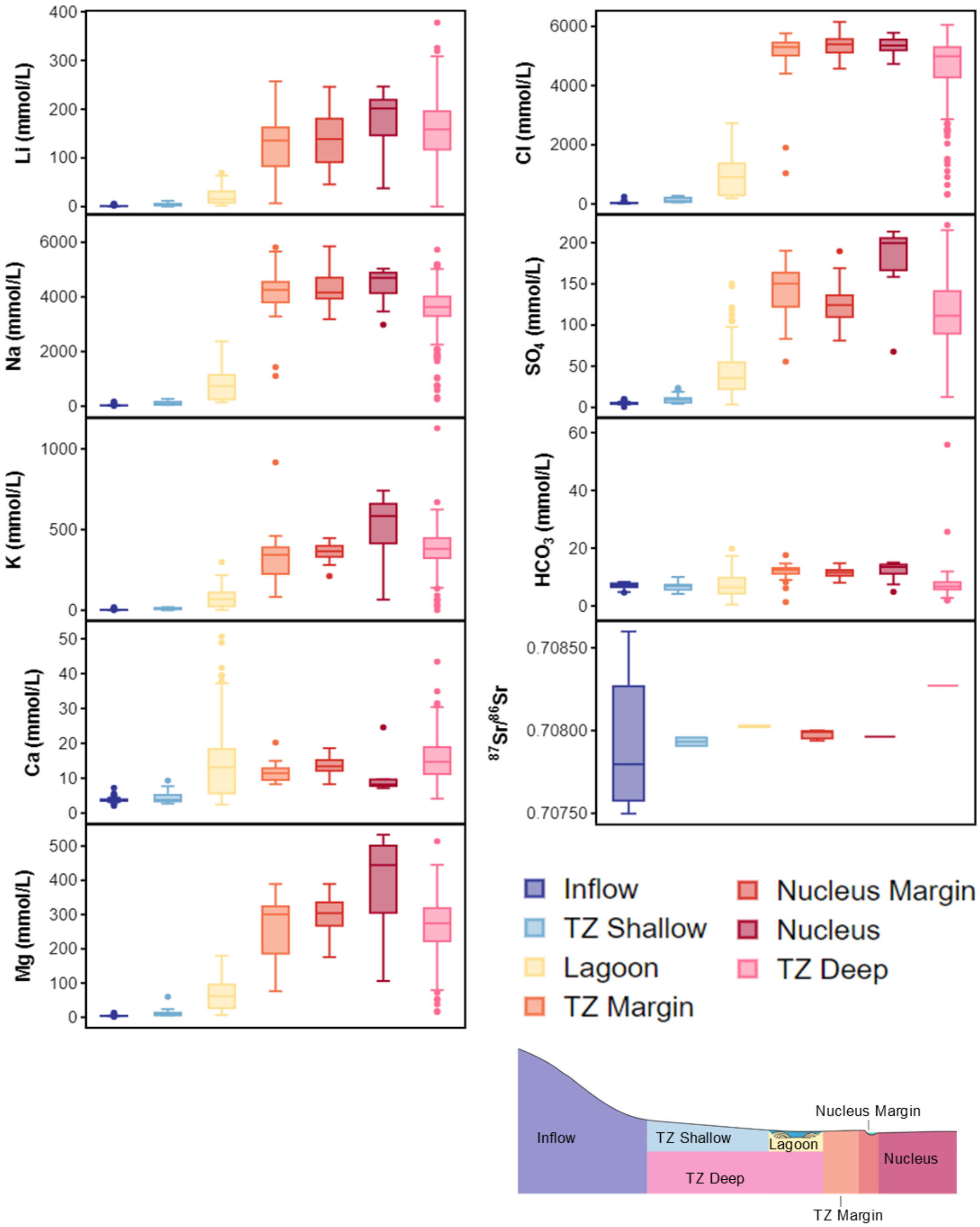

Figure 5. Chemical composition of major cations and anions and $^{87}Sr/^{86}Sr$ signatures in all water compartments including all sampling events for this study. Inset representative cross section simplified from the conceptual model in Figure 3.

aquifer materials could be altered significantly. The analysis performed in the current work has the objective of using natural water chemistry and testing which minerals are at or near equilibrium to confirm our observations of secondary mineral precipitation in surficial deposits and those from the diamond drill cores in the subsurface of the southern transition zone.

Figure 6 illustrates the results of the equilibrium geochemical modeling for all of the water zones along the southern margin of the SdA transect into the halite nucleus for calcite, gypsum and halite. The data used for this modeling were split into those with ionic strength < 0.1 and those with ionic strength > 0.1 (Table S1). The lower and intermediate ionic strength waters modeled include those from the inflow and the transition zone and therefore produce results that include not only the common evaporite minerals of carbonates, sulfates and chlorides but also some silicates as the activity of $SiO_{2(aq)}$ is high enough in these regions. There are some 1-5 cm lenses of dense chert-like material that appear to be post depositional which are found within the cores in the transition zone. A sample of this material has been identified as containing trydimite by XRD methods (J. Grotzinger, pers. comm.). The results from the inflow water modeling are similar to those for inflow waters found further upgradient by 10s of km in the same aquifer (MNT) as reported in Rissmann et al. (2015) (discussed in S1). For waters in the lagoons, TZ margin, nucleus margin, and halite nucleus, we report the range of saturation indices for calcite, gypsum and halite as those are the dominant mineral phases observed in the field from surface mapping and in the subsurface from drill core (up to 200 m).

Along the flow path the general trend indicates that the inflow and transition zone waters are undersaturated with respect to halite and gypsum (log Q/K < 0) but are at saturation with respect to calcite (log Q/K > 0) and other carbonate, sulfate and silicate minerals (Table S1). The lagoon waters which are represented here by waters from Laguna Brava are undersaturated with respect to halite but are at saturation with respect to calcite and to a lesser extent gypsum. The TZ margin, nucleus margin, and the nucleus waters are all saturated with respect to halite, gypsum and calcite indicating that it is in these regions that concentrations/activities of the required ions are elevated enough to cause the precipitation of all mineral phases. It is also apparent that the lagoon, transition zone, and nucleus edge waters have the most range in SI values which is expected because these waters are more susceptible to precipitation events and evaporation given that they are exposed at the surface or contain components of water that are exposed at the surface.

Note that in the field there are areas within the transition zone that display vadose zone processes are at work including formation of secondary mineral precipitates such as efflorescent salts and chlorides that are precipitating within cracks and other openings in the primary salt crusts. We attribute these to evaporation processes and the continual delivery of solutes above the water table to form these secondary minerals.

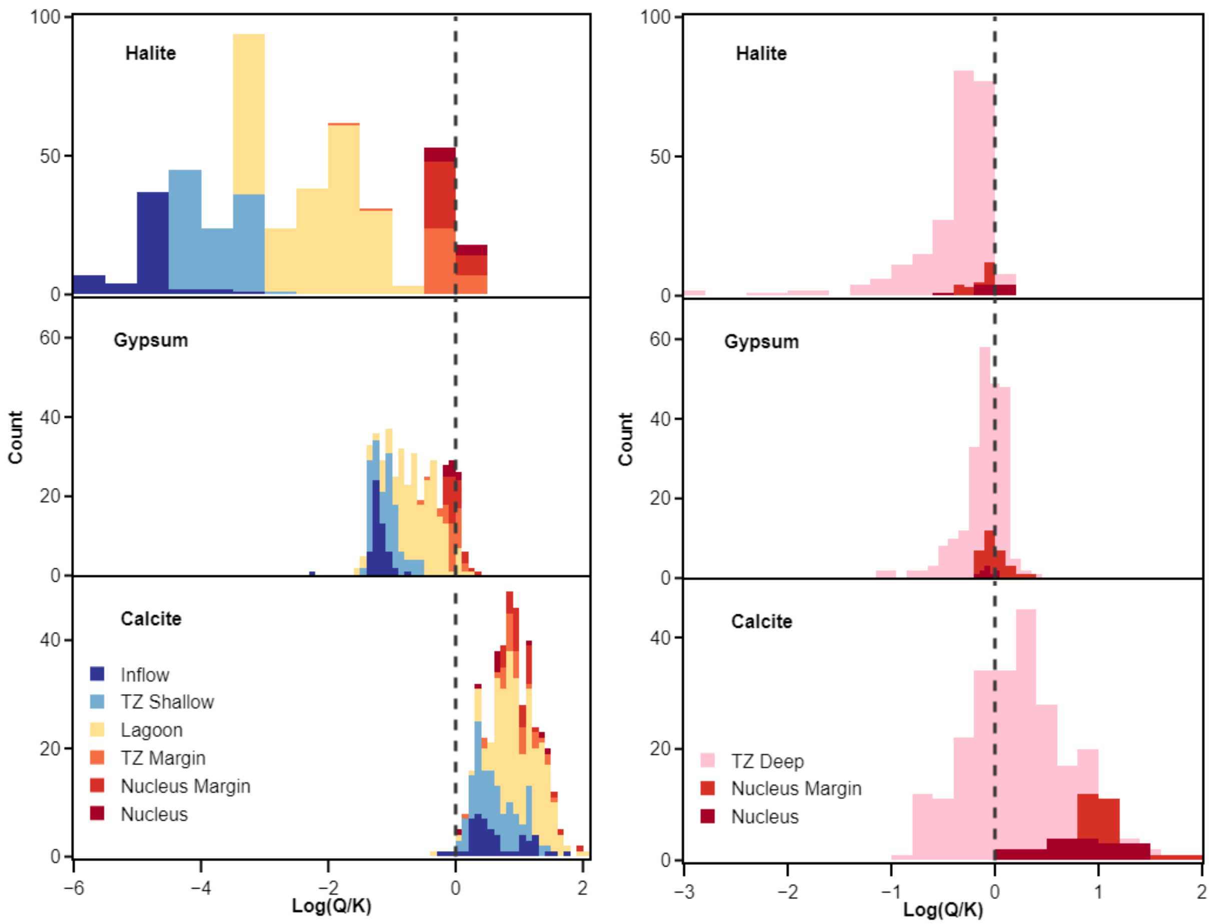

Figure 6. Histograms of predicted Log (Q/K) saturation indices for major evaporite phases for all of the water compartments in the SdA inflow-transition zone- nucleus system including subsurface brines found under the transition zone (TZ deep) for multi-year/seasonal data. All modeled SI data are included in Table S1.

4.3 Temporal Dynamics of Open Pool and Lagoon Waters

The margin of the halite nucleus along the southern margin of SdA is characterized by a ~ 2 m wide depression that fills with water from precipitation events on or near the salar surface, these features are defined as the open pools (Boutt et al., 2016). The open pools form from the dissolution of the halite primarily by fresher rain water (^{3}H observations from Boutt et al., 2016 and Figure 4) and likely from smaller amounts of shallow locally-derived groundwater emerging from alluvial fans on the west and east side of the Cordon de Lila. Over time the water in the depression evaporates resulting in stable water isotopic signatures that are highly enriched (Boutt et al., 2016) as the pools frequently evaporate to complete dryness during the austral summer which is accompanied by precipitation of secondary minerals including halite. Figure 7 illustrates the southern margin of SdA from 1969-2014. It is compiled from the oldest published geologic map (Morega et al., 1969) that depicts the open pools combined with the January 2014 Landsat image. The outline of the position of the edge of the nucleus margin/open pools is based on the 1969 map, the 1999 position and the 2014 position from Landsat imagery. The results of this analysis indicate two important observations 1) the open pool features have persisted through time at least back to 1969 prior to the onset of any brine extraction and 2) the most change to the position of the nucleus edge occurred between 1969 and 1999 and little change is detectable between 1999 and 2014.

Satellite imagery and geochemical and isotopic analyses of lagoon waters indicate that the lagoons are seasonally dynamic features that are supported by shallow groundwater discharge but also respond to local precipitation events (Boutt et al., 2016). Figure 8a. depicts the surface area extent of surface water bodies in the southern transition zone before and after a major precipitation event that occurred on the salar in March 26, 2015. The result was a growth in surface area of all the surface water features by a factor of 2.7. Lagoon surface area extent changed from 0.9 km^2 to 1.6 km^2, an increase of 77% which is about 25% higher than the change over an annual cycle caused by incident solar radiation. The open pools grew by over 250% after the precipitation event changing in size from 0.33 km^2 to 1.28 km^2.

The longer term (2002-2016) annual variation in surface area of both the PBLC and SSI lagoons and the open pools along the nucleus margin as well as daily precipitation recorded at the DGA Peine meteorological station (located on the southeast of the Salar) are illustrated in Figure 8b. These changes were first highlighted by Boutt et al. (2016) but are also demonstrative in this analysis because these observations indicate the annual and decadal dynamic behavior of the surface water bodies in the transition zone. Overall the SSI lagoon system appears to have the least amount of natural variability as compared to the PBLC system and the open pools along the nucleus margin, which highlights the importance of investigating and monitoring each lagoon system and other groundwater discharge or precipitation influenced features over time in order to have the most robust picture of change. This type of analysis combined with other ground truthing is fundamental in the overall understanding of water use and its impacts in this basin. For example, in order to really assess the impact of groundwater pumping of brine or freshwater on the surface water bodies, the natural responses of these water bodies to regular hydrologic events provides the baseline from which to assess other impacts.

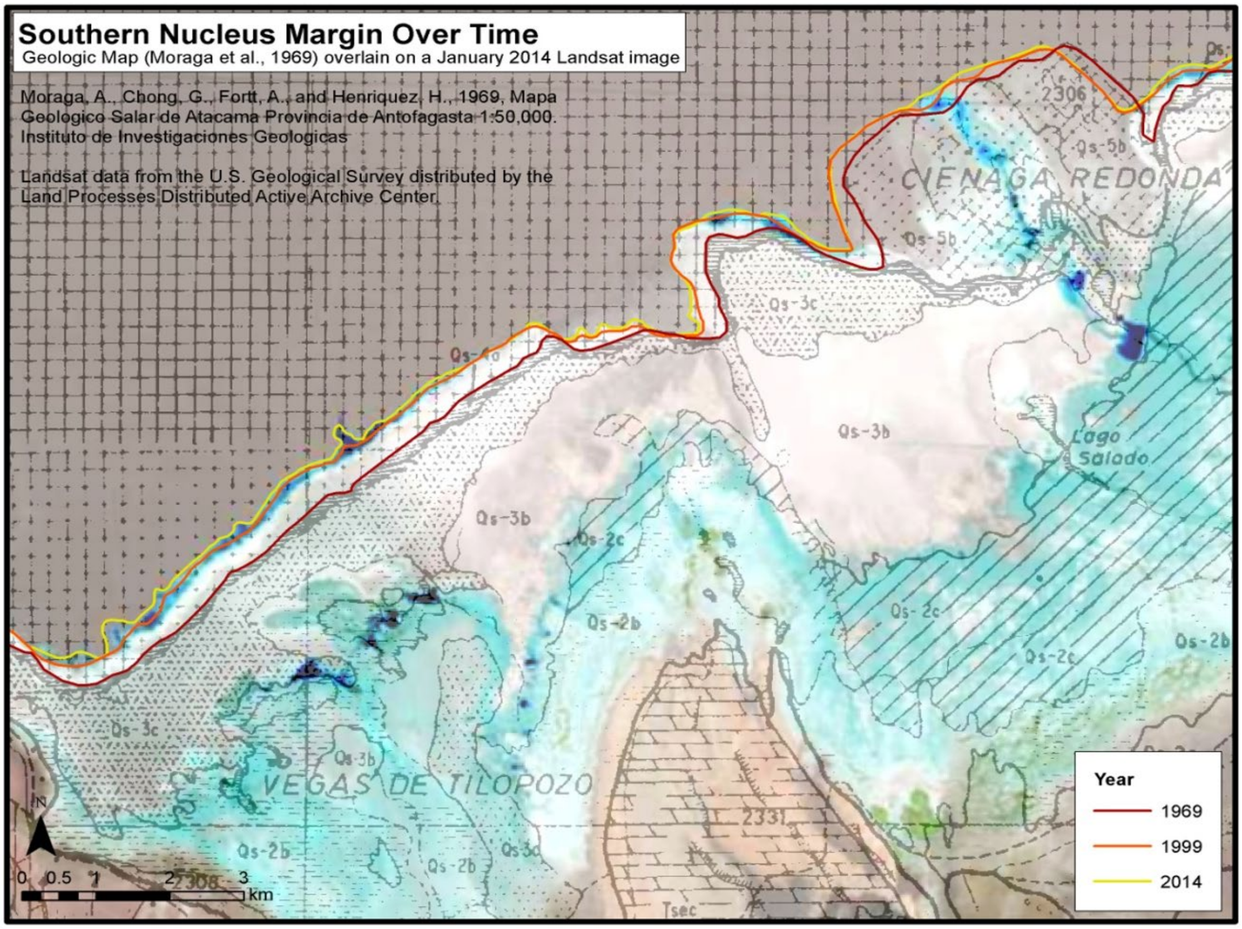

Figure 7. Section of the geologic map from Moraga et al. (1969) for the southeast part of SdA overlain on the January 2014 Landsat image. The position of the nucleus edge where the open pools accumulate and evaporate in 2014 is outlined in yellow as well as the positions of this same feature in 1999 (orange) and 1969 (red). Mapped geologic unit abbreviations can be found in Moraga et al. (1969).

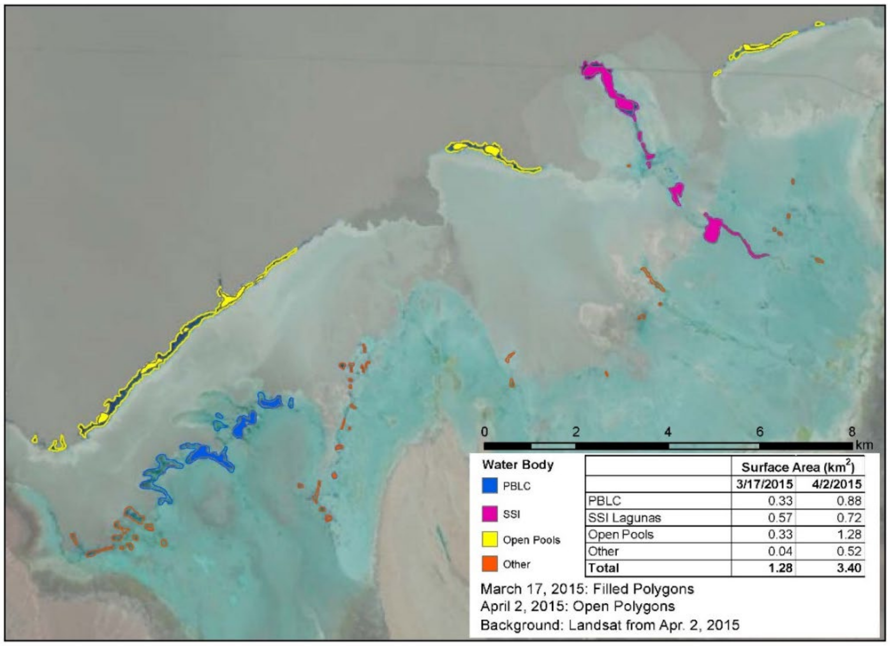

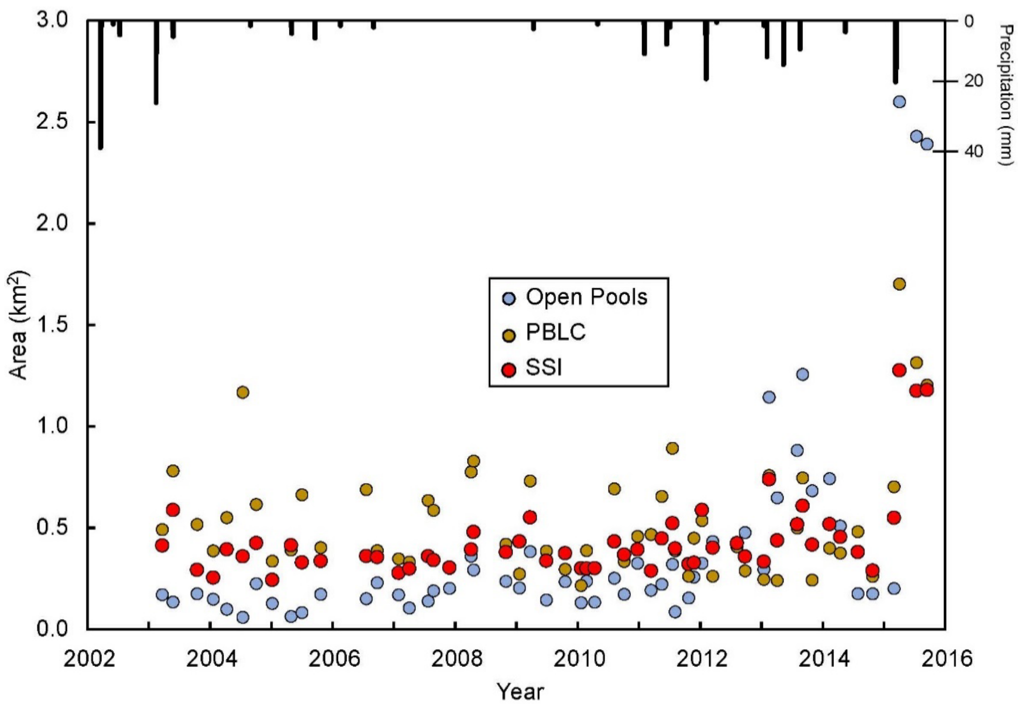

Figure 8a-b. Top panel (a) Landsat image from April 2, 2015 depicting the change in the surface area of surface water bodies in the TZ, TZ margin, lagoons, and nucleus edge before and after a major storm event in March 2015. Lower panel (b) is the long-term changes in surface area of the open pools and two lagoon systems in the southern SdA area as determined from remote sensing mapping of based on Landsat imagery.

5 Discussion

5.1 Flow Path Evolution

The water discharging in the vicinity of the lagoons flows along long flow paths discharging from the inflow region into the TZ shallow zone (Figure 3). As water enters this region it begins to undergo a physical and chemical transformation due to the proximity of the water with the land surface. Evaporation, mineral precipitation, and dissolution cause the water to increase in TDS. Flow paths into the region have both a horizontal and vertical component to them as depicted with arrows in Figure 3. The presence of evaporate deposits with varying permeabilities causes the flow paths to converge on the TZ shallow region until they reach 1-2 m below ground surface. At this depth, evaporation begins to remove water from the system driving mineral precipitation in the order of carbonate in the marshes and further salarward additional equilibrium with gypsum and halite is reached. There are a number of discrete flow paths into the TZ shallow zone that discharge at varying rates and locations throughout this area. Some of the water forms springs that discharge at rates greater than the rate at which evaporation can remove the water into the atmosphere. Water does not pool everywhere on the surface in this zone for two reasons: 1) discharge appears to be smaller than the soil evaporation and 2) once water is present at the surface evaporation rates increase substantially resulting in a non-linear feedback. Because evaporation varies seasonally, some seeps with lower inflow rates are ephemeral and form small lagoons that are seasonally present. The predominant discharge locations occur in the regions up hydraulic gradient of the lagoons. Here the discharge rates are high enough that the rate of discharge greatly exceeds evaporation forming large perennial surface water features which are the lagoons. While there are local seeps in and around the margin of lagoons, the majority of water flux into the lagoons appears to be upgradient of the actual surface water feature. Boutt et al. (2016) and Moran et al. (2019) showed that water discharging to these lagoons is a complex mixture of regional groundwater and modern precipitation, further the results presented here indicate considerable seasonal variability in the geochemistry of the lagoon waters. Tritium analyses of lagoon waters show that the lagoons at any one time can have up to 30% modern water highlighting the importance of sporadic precipitation events on the hydrologic budget of the lagoons, even though over the long term most of the water is sourced from older regional flow paths (Boutt et al., 2016).

5.2 Geochemical Evolution of Waters in Transition Zone

The physical and chemical transect of the shallow inflow, TZ shallow, lagoons, TZ margin, nucleus margin, and nucleus in Figure 4 indicates that the shallow groundwater system evolves from fresh to brackish to brine waters over a long flow path originating in the upgradient MNT aquifer which is the primary source of inflow water. Previously, Munk et al. (2018, Fig. 8) demonstrated that the lithium brine in the nucleus is formed over timeframes of millions of years from water-rock interaction in the inflow zones followed by concentrating processes of evaporation and ultimately by halite fractional crystallization causing the residual brines to become highly enriched in Li which is extremely incompatible. The work presented in this contribution further exemplifies that the TZ regions of salars are unique and independent hydrogeologic functioning areas that are decoupled from the thick less hydrogeologically active nucleus. This is demonstrated by the lack of hydrogeochemical connection between the lagoons, the TZ margin, and the nucleus margin waters (Figure 4). Recharge to the halite nucleus does happen (Boutt et al., 2016) but is primarily through waters that accumulate along the halite nucleus margin in open pools as well as through direct precipitation on the salar surface. Recent work on developing 3D geologic and hydrostratigraphic models of the SdA basin has led to additional evidence to support that major faults in the region may also move fluids into and within the halite nucleus, however, that hypothesis is still under consideration and requires further testing.

The major cation and anion plus Li concentration data for all of the defined water zones in the inflow-transition zone-nucleus system further illustrate the lack of similarity between the inflow and TZ shallow waters as compared to the lagoons, and the TZ margin, nucleus margin, TZ deep and the nucleus waters (Figure 5). The compartments that appear to have geochemical cohesion are 1) the inflow and shallow TZ, 2) lagoons, 3) TZ margin, TZ deep and nucleus margin, and 4) nucleus. Munk et al. (2018) indicated that the difference between the inflow/TZ shallow waters and the lagoons could easily be explained by evaporation of the inflows to reach concentrations observed in the lagoons, which holds in this expanded dataset as well. However, the current analysis also indicates that the waters salarward of the lagoons and upgradient of the nucleus also are distinct in this system but similar to each other whereas the nucleus brines have their own geochemical signature and are distinct from the TZ brines. The $^{87}Sr/^{86}Sr$ signatures indicate that there is subsurface weathering/dissolution water-rock interaction with a more radiogenic source, likely the Tucucaro ignimbrite or other volcanic deposits. Not only is this subsurface process likely a major way Li and other elements are released to the brine but also contributes to increasing the porosity and permeability of the ignimbrite as a potential aquifer.

There are two critical findings from this data and analysis: 1) the inflow and TZ shallow waters are distinct from a subsurface brine that occurs in the TZ deep, 2) the TZ deep brines are geochemically distinct from the nucleus brines indicating that overall the TZ appears to be hydrogeologically distinct from the nucleus in both the shallow groundwater system and the deeper brine groundwater system. McKnight et al. (2020) build on these ground-truthed observations to further model the decoupling of the freshwater-brine interface and demonstrating that it is critical to use heterogenous modeling approaches to best represent these systems. The new detailed subsurface geology that has been interpreted (Figure 3) also supports these findings given the large range of hydraulic conductivities of this aquifer system.

The results of the geochemical equilibrium modeling presented in Figure 6 indicate that there are definitive zones of predictable mineral precipitation in the inflow-transition-nucleus system but that there is considerable variability particularly in surface water bodies directly exposed to the influence of evaporation. Halite saturation is apparent only in the nucleus, nucleus margin, TZ margin and some of the TZ deep brines. Gypsum saturation occurs within those same waters but also in some lagoon waters and calcite saturation occurs across all water zones. The TZ deep brines are also distinct from other brines in the system showing a much larger variability in geochemical composition and predicted saturation states. The later finding is critical as TZ brines have not yet been rigorously studied and as they appear to be distinct from the nucleus brines there maybe additional/different processes responsible for their formation. The equilibrium modeling also aids in verifying the role of secondary mineral precipitation on the hydrogeologic properties of porosity and permeability in the aquifer system of the TZ as depicted in Figure 3.

5.3 Spatial and Temporal Dynamics of Groundwater Discharge Features and Open Pools

The hydrodynamic behavior of the lagoon systems in the transition zone is dependent on support from groundwater discharge derived upgradient, annual fluctuations in evaporation and direct precipitation on the salar. The open pools along the halite nucleus margin have a distinct hydrodynamic behavior from that of the other open bodies of water in the transition zone because they are not supported by continued groundwater discharge but rather respond to precipitation events on the salar surface. This is a major distinction between the lagoons and the open pools indicating their general lack of hydraulic connection. The remote sensing analysis of the open bodies of water in the transitional areas of the salar further reveal the importance of precipitation events and climate on the size of these water bodies.

6 Conclusions

This work is the first to quantify the relationship between the hydrogeological and geochemical zones of salar freshwater-brine systems. A pivotal finding from this research is that complex subsurface geology and the development of a freshwater-brine interface control the formation of the defined water zones. These important observations made through a complete assessment of all water types through the salar freshwater-brine system is supported by physical, geologic, geochemical, and isotopic evidence. The sustainability of the nucleus brine and freshwater resources in this region is dependent on this rigorous scientific analysis. These new observations and findings are particularly important in understanding the position and dynamic behavior of lagoons and other surface water bodies in the transitional zone of salar systems. The lagoons grow and shrink in response to climate and precipitation, are perched by low permeability materials in the subsurface and are dependent on freshwater inflow from the southern aquifers (MNT), not on the position of the freshwater-brine interface in the subsurface. Geochemical differences in the transition zone brine and the nucleus brine indicate that there may be other processes responsible for the formation of the TZ brine as compared to the nucleus brine.

7 Acknowledgments and Data

The authors would like to thank Albemarle for providing access to diamond drill cores for analysis as well as access to their internal database of water chemistry and for general support of the research, particularly for field operations. Contributions from Lilly Corenthal, Leah Santangelo, and Anna Campbell are gratefully acknowledged with remote sensing analysis presented here. This project was also partially supported by NSF award 1443226. There are no real or perceived financial conflicts or interests for any of the authors. Data supporting the conclusions can be obtained from https://doi.org/10.7275/qr40-z439.

References

Allmendinger, R. W., Jordan, T. E., Kay, S. M., & Isacks, B. L. (1997). The Evolution of The Altiplano-Puna Plateau of the Central Andes. Annual Review of Earth and Planetary Sciences, 25(1), 139–174. https://doi.org/10.1146/annurev.earth.25.1.139

Aron, F., González, G., Veloso, E., & Cembrano, J. (2008). Architecture and style of compressive Neogene deformation in the eastern-southeastern border of the Salar de Atacama Basin (22 30'-24 15'S): A structural setting for the active volcanic arc of the Central Andes. In 7th International Symposium on Andean Geodynamics (ISAG 2008, Nice) (pp. 52-55)

Boschetti, T., Cortecci, G., Barbieri, M., & Mussi, M. (2007). New and past geochemical data on fresh to brine waters of the Salar de Atacama and Andean Altiplano, northern Chile. Geofluids, 7(1), 33-50.

Boutt, D., Corenthal, L., Munk, L. A., & Hynek, S. (2018). Imbalance in the modern hydrologic budget of topographic catchments along the western slope of the Andes (21–25 S). https://doi.org/10.31223/osf.io/p5tsq

Breitkreuz, C. (1995). The late Permian Peine and Cas Formations at the eastern margin of the Salar de Atacama, Northern Chile: stratigraphy, volcanic facies, and tectonics. Revista Geológica de Chile, 22(1), 3–23.

Cervetto Sepúlveda, M. M. (2012). Caracterización hidrogeológica e hidrogeoquímica de las cuencas: Salar de Aguas calientes 2, Puntas negras, Laguna Tuyajto, Pampa Colorada, Pampa Las Tecas y Salar el Laco, II región de Chile.

Chaffaut I, Coudrain-Ribstein A, Michelot JL, Pouyaud B. (1998) Precipitations d'altitude du Nord-Chili, origine des sources de vapeur et donnees isotopiques. Bulletin de l'Institute Francais d etudes andine, 27, 367–84.

de Silva, S. L. (1989). Geochronology and stratigraphy of the ignimbrites from the 21°30′S to 23°30′S portion of the Central Andes of northern Chile. *Journal of Volcanology and Geothermal Research*, *37*(2), 93–131. https://doi.org/10.1016/0377-0273(89)90065-6

de Silva, S. L. (1989a). Altiplano-Puna volcanic complex of the central Andes. *Geology*, *17*(12), 1102–1106. https://doi.org/10.1130/0091-7613(1989)017<1102:APVCOT>2.3.CO;2

Gardeweg, M., & Ramírez, C. F. (1987). La Pacana caldera and the Atana Ignimbrite - a major ash-flow and resurgent caldera complex in the Andes of northern Chile. Bulletin of Volcanology, 49(3), 547–566. https://doi.org/10.1007/BF01080449

Gleeson, T., Cuthbert, M., Ferguson, G., & Perrone, D. (2020). Global Groundwater Sustainability, Resources, and Systems in the Anthropocene. Annual Review of Earth and Planetary Sciences, 48(1), 431–463. https://doi.org/10.1146/annurev-earth-071719-055251

González, G., Cembrano, J., Aron, F., Veloso, E. E., & Shyu, J. B. H. (2009). Coeval compressional deformation and volcanism in the central Andes, case studies from northern Chile (23°S-24°S). Tectonics, 28(6). https://doi.org/10.1029/2009TC002538

Herrera, C., Custodio, E., Chong, G., Lambán, L. J., Riquelme, R., Wilke, H., … Lictevout, E. (2016). Groundwater flow in a closed basin with a saline shallow lake in a volcanic area: Laguna Tuyajto, northern Chilean Altiplano of the Andes. Science of the Total Environment, 541, 303–318. https://doi.org/10.1016/j.scitotenv.2015.09.060

Houston, J. (2009). A recharge model for high altitude, arid, Andean aquifers. Hydrological Processes, 23(16), 2383–2393. https://doi.org/10.1002/hyp.7350
Houston, J., Butcher, A., Ehren, P., Evans, K., & Godfrey, L. (2011, November). The evaluation of brine prospects and the requirement for modifications to filing standards. Economic Geology. https://doi.org/10.2113/econgeo.106.7.1225
Houston, J. & Hart, D. (2004). Theoretical head decay in closed basin aquifers: an insight into fossil groundwater and recharge events in the Andes of northern Chile. Quarterly Journal of Engineering Geology and Hydrogeology 37, 131–139. doi:10.1144/1470-9236/04-007
Jordan, T. E., L. V. Godfrey, N. Munoz, R. N. Alonso, T. K. Lowenstein, G. D. Hoke, N. Peranginangin, B. L. Isacks, and L. Cathles (2002), Orogenic-scale ground water circulation in the Central Andes: evidence and consequences., 5th ISAG (International Symp. Andean Geodyn.), 331–334.
Jordan, T. E., Mpodozis, C., Muñoz, N., Blanco, N., Pananont, P., & Gardeweg, M. (2007). Cenozoic subsurface stratigraphy and structure of the Salar de Atacama Basin, northern Chile. Journal of South American Earth Sciences, 23(2–3), 122–146. https://doi.org/10.1016/j.jsames.2006.09.024
Jordan, T. E., Nester, P. L., Blanco, N., Hoke, G. D., Dávila, F., & Tomlinson, A. J. (2010). Uplift of the Altiplano-Puna plateau: A view from the west. Tectonics, 29(5). https://doi.org/10.1029/2010TC002661
Kuhn, D. (2002). Fold and thrust belt structures and strike-slip faulting at the SE margin of the Salar de Atacama basin, Chilean Andes. Tectonics, 21(4), 8-1-8–17. https://doi.org/10.1029/2001TC901042
Martínez, F., López, C., Bascuñan, S., & Arriagada, C. (2018). Tectonic interaction between Mesozoic to Cenozoic extensional and contractional structures in the Preandean Depression (23°–25°S): Geologic implications for the Central Andes. Tectonophysics, 744, 333–349. https://doi.org/10.1016/j.tecto.2018.07.016
McKnight, S., Boutt, D., & Munk, L. A. (2020, July 10). Impact of Hydrostratigraphic Continuity in Heterogeneity on Brine-to-Freshwater Interface Dynamics; Implications from a 2-D Parametric Study in an Arid and Endorheic Basin. https://doi.org/10.31223/osf.io/ea783
Mather, A. E., & Hartley, A. (2005). Flow events on a hyper-arid alluvial fan: Quebrada Tambores, Salar de Atacama, northern Chile. Geological Society Special Publication, 251, 9–24. https://doi.org/10.1144/GSL.SP.2005.251.01.02
Moran, B. J., Boutt, D. F., & Munk, L. A. (2019). Stable and Radioisotope Systematics Reveal Fossil Water as Fundamental Characteristic of Arid Orogenic-Scale Groundwater Systems. Water Resources Research, 55(12), 11295–11315. https://doi.org/10.1029/2019WR026386
Ortiz, C., Aravena, R., Briones, E., Suárez, F., Tore, C., & Muñoz, J. F. (2014). Sources of surface water for the Soncor ecosystem, Salar de Atacama basin, northern Chile. Hydrological Sciences Journal, 59(2), 336-350.
Pigati, J. S., Rech, J. A., Quade, J., & Bright, J. (2014, May). Desert wetlands in the geologic record. Earth-Science Reviews. https://doi.org/10.1016/j.earscirev.2014.02.001
Reutter, K. J., Charrier, R., Götze, H. J., Schurr, B., Wigger, P., Scheuber, E., ... & Chong, G. (2006). The Salar de Atacama Basin: a subsiding block within the western edge of the Altiplano-Puna Plateau. In the Andes (pp. 303-325). Springer Berlin Heidelberg.
Risacher, F., Alonso, H., Salazar, C. (1999). Geoquímica de aguas en cuencas cerradas: I, II y III Regiones–Chile. 1. Ministerio de Obras Públicas, pp. 209.
Rissmann, C., Leybourne, M., Benn, C., & Christenson, B. (2015). The origin of solutes within the groundwaters of a high Andean aquifer. Chemical Geology, 396, 164–181. https://doi.org/10.1016/j.chemgeo.2014.11.029
Rosen, M. R. (1994). The importance of groundwater in playas: A review of playa classifications and the sedimentology and hydrology of playas. Special Paper of the Geological Society of America, 289, 1–18. https://doi.org/10.1130/SPE289-p1
Rubilar, J., Martínez, F., Arriagada, C., Becerra, J., & Bascuñán, S. (2018). Structure of the Cordillera de la Sal: A key tectonic element for the Oligocene-Neogene evolution of the Salar de Atacama basin,

Central Andes, northern Chile. Journal of South American Earth Sciences, 87, 200–210. https://doi.org/10.1016/j.jsames.2017.11.013

Strecker, M. R., Alonso, R. N., Bookhagen, B., Carrapa, B., Hilley, G. E., Sobel, E. R., & Trauth, M. H. (2007). Tectonics and Climate of the Southern Central Andes. Annual Review of Earth and Planetary Sciences, 35(1), 747–787. https://doi.org/10.1146/annurev.earth.35.031306.140158

Tyler, S. W., Muñoz, J. F., & Wood, W. W. (2006). The response of playa and sabkha hydraulics and mineralogy to climate forcing. Ground Water. https://doi.org/10.1111/j.1745-6584.2005.00096.x

Wang, J., Song, C., Reager, J. T., Yao, F., Famiglietti, J. S., Sheng, Y., … Wada, Y. (2018). Recent global decline in endorheic basin water storages. Nature Geoscience, 11(12), 926–932. https://doi.org/10.1038/s41561-018-0265-7

Ward, K. M., Zandt, G., Beck, S. L., Christensen, D. H., & McFarlin, H. (2014). Seismic imaging of the magmatic underpinnings beneath the Altiplano-Puna volcanic complex from the joint inversion of surface wave dispersion and receiver functions. Earth and Planetary Science Letters, 404, 43–53. https://doi.org/10.1016/j.epsl.2014.07.022

Warren, J. K. (2010). Evaporites through time: Tectonic, climatic and eustatic controls in marine and nonmarine deposits. Earth-Science Reviews. https://doi.org/10.1016/j.earscirev.2009.11.004

Warren, J. (2015). Evaporites A Geological Compendium Second Edition. Evaporites A Geological Compendium Second Edition (pp. 1–3). https://doi.org/10.1007/978-3-319-13512-0

Wilson, J. L., & Guan, H. (2013). Mountain-Block Hydrology and Mountain-Front Recharge. In Groundwater Recharge in a Desert Environment: The Southwestern United States (Vol. 9, pp. 113–137). American Geophysical Union. https://doi.org/10.1029/009WSA08

WMC [Water Management Consultants Ltda.] (2007). Analisis de la relacion entre las aguas subterraneas del Proyecto Pampa Colorada, las vertientes y del margen este del Salar de Atacama y las Lagunas Miscanti y Minique, Informe III Final, Santiago, Chile.

Zipper, S. C., Jaramillo, F., Wang-Erlandsson, L., Cornell, S. E., Gleeson, T., Porkka, M., … Gordon, L. (2020). Integrating the Water Planetary Boundary With Water Management From Local to Global Scales. Earth's Future, 8(2). https://doi.org/10.1029/2019ef001377

AGU PUBLICATIONS

Geophysics, Geochemistry, Geosystems

Supporting Information for

Hydrogeologic and Geochemical Distinctions in Salar Freshwater Brine Systems

L. A. Munk[1] 0000-0003-2850-545X, D. F. Boutt[2] 0000-0003-1397-0279, B. J. Moran[2] 0000-0002-9862-6241, S. V. McKnight[2] 0000-0002-6013-193X, J. Jenckes[1] 0000-0002-1811-3076

[1]Department of Geological Sciences, University of Alaska Anchorage

[2]Department of Geosciences, University of Massachusetts Amherst

Corresponding author: Lee Ann Munk (lamunk@alaska.edu)

Contents of this file

Additional Supporting Information (Files uploaded separately)

Introduction

The supporting information contained in this section includes results from geochemical equilibrium modeling of the different water types analyzed in this paper for each of the hydrogeologic zones defined. These modeling results were used to produce figure 6 in the main text and all of the raw data are included at https://doi.org/10.7275/qr40-z439. Geochemist Workbench was used to produce these modeled results of saturation indices with the ionic strength approximation used for each sample based on the ionic strength of the solution (greater than or less than 0.1). Saturation indices values below 1.0 indicate undersaturation and values at or above 1.0 indicate saturation based on thermodynamic data and temperature of each sample. Inflow waters with lower ionic strength were modeled with the Debye-Huckel approximation and brackish waters and brines were modeled with the Harvie-Moller-Weare approximation.

In addition to the results illustrated in Figure 6 for the major evaporite minerals, other minerals are also predicted to be at or near saturation in the inflow and TZ shallow zone water including aragonite ($CaCO_3$), dolomite (($Ca,Mg)CO_3$), strontianite ($SrCO_3$), witherite ($BaCO_3$), barite ($BaSO_4$), amorphous silica ($SiO_{2(am)}$), chalcedony (SiO_2), and cristobalite (SiO_2).

Celestite ($BaSO_4$) is predicted to be undersaturated in all water zones. Anhydrite is also predicted as undersaturated in all water zones which is consistent with our observations that this mineral although present is very sparse in outcrop and diamond drill cores recovered from the transition zone and the nucleus. Antarcticite ($CaCl*6H_2O$) is included in the modeling results and is undersaturated in all waters analyzed.

Saturation indices are blank in Table S1 where elemental concentration data were not available.

Table S1. Modeled saturation indices for all water types and samples used in the analysis.

A virtual field trip movie is included to aid in the reader's experience and understanding of the environment and defined water zones in this study. The major water zones and some of the important surface water bodies are identified with text in the movie, these correspond with the zones and features referred to in the text. Enjoy.

Movie S1. Drone video of the newly identified hydrogeologic and geochemical zones of the Salar de Atacama.

Sample_ID	Zone	Sample_ Date	Calcite	Gypsum	Halite	Aragonite	Dolomite	Strontianite	Witherite	Barite	Amorphous silica	Chalcedony	Cristobalite	Celestite	Anhydrite	Antarcticite	Activity Coefficient Approximation
138	Inflow	2/21/13	0.326	-1.343	-5.886	0.162	1.635	0.822			-0.182	0.832	0.553	-1.649	-1.515	-11.600	Debye-Huckel
138	Inflow	5/23/13	0.873	-1.206	-5.532	0.708	2.581	1.819			0.320	1.350	1.068	-1.090	-1.401	-11.020	Debye-Huckel
138	Inflow	7/27/13	0.291	-1.199	-5.531	0.127	1.446				-0.948	0.068	-0.211		-1.374	-11.050	Debye-Huckel
138	Inflow	9/8/13	0.384	-1.205	-5.491	0.220	1.630	1.038			-0.018	0.987	0.710	-1.334	-1.363	-11.080	Debye-Huckel
138	Inflow	10/17/13	0.349	-1.171	-5.555	0.184	1.506	1.051			-0.122	0.911	0.628	-1.306	-1.370	-11.030	Debye-Huckel
138	Inflow	11/29/13	0.300	-1.147	-5.551	0.135	1.484	1.040			-0.035	0.994	0.712	-1.237	-1.341	-11.000	Debye-Huckel
138	Inflow	12/10/13	0.515	-1.265	-5.548	0.350	1.929	1.386			-0.027	0.996	0.715	-1.212	-1.450	-11.120	Debye-Huckel
138	Inflow	1/22/14	0.316	-1.250	-5.442	0.151	1.541	0.974			-0.083	0.927	0.648	-1.383	-1.414	-11.040	Debye-Huckel
138	Inflow	2/14/14	-0.201	-1.314	-5.687	-0.365	0.658	0.800			-0.114	0.874	0.600	-1.061	-1.445	-11.250	Debye-Huckel
200	Inflow	10/22/13	0.582	-1.148	-4.693	0.418	2.186	1.080			-0.151	0.845	0.569	-1.414	-1.291	-10.010	Debye-Huckel
200	Inflow	12/17/13	0.078	-1.237	-4.881	-0.086	1.173	0.877			-0.228	0.763	0.488	-1.193	-1.373	-10.310	Debye-Huckel
200	Inflow	1/14/14	0.469	-1.250	-4.782	0.305	1.888	0.473						-2.031	-1.410	-10.230	Debye-Huckel
200	Inflow	2/14/14	-0.091	-1.283	-5.000	-0.256	0.812	0.969			-0.069	0.941	0.663	-1.016	-1.449	-10.430	Debye-Huckel
200	Inflow	3/18/14	0.417	-1.191	-4.905	0.253	1.793	0.831	0.710	-0.085	0.022	1.032	0.754	-1.569	-1.356	-10.150	Debye-Huckel
200	Inflow	4/19/14	0.561	-1.183	-4.888	0.396	2.087	0.960	0.943	0.012	0.004	1.014	0.736	-1.575	-1.348	-10.170	Debye-Huckel
200	Inflow	5/14/14	0.268	-1.076	-4.970	0.104	1.484	0.689	0.617	0.082	-0.069	0.944	0.665	-1.455	-1.246	-10.360	Debye-Huckel
200	Inflow	6/14/14	0.182	-1.202	-4.949	0.017	1.267	0.625	0.479	-0.105	-0.038	0.983	0.703	-1.572	-1.383	-10.320	Debye-Huckel
200	Inflow	7/21/14	0.272	-1.238	-4.715	0.107	1.529	0.686	0.634	-0.070	-0.060	0.956	0.677	-1.627	-1.412	-10.060	Debye-Huckel
200	Inflow	8/19/14	0.314	-1.269	-4.614	0.149	1.627	0.740	0.709	-0.069	-0.098	0.919	0.640	-1.649	-1.444	-9.938	Debye-Huckel
200	Inflow	9/7/14	0.612	-1.164	-4.644	0.447	2.234	1.052	0.998	0.027	-0.094	0.923	0.643	-1.529	-1.339	-10.020	Debye-Huckel
200	Inflow	10/11/14	0.529	-1.015	-4.523	0.365	1.930	0.763	0.713	-0.021	-0.112	0.901	0.622	-1.577	-1.183	-9.645	Debye-Huckel
200	Inflow	11/4/14	0.356	-1.173	-4.698	0.192	1.735	0.774	0.719	0.002	-0.105	0.905	0.627	-1.549	-1.339	-10.090	Debye-Huckel
200	Inflow	12/5/14	0.404	-2.284	-4.494	0.239	1.897	0.906	1.148	-0.735	0.049	1.065	0.786	-2.586	-2.458	-9.783	Debye-Huckel
200	Inflow	1/11/15	0.758	-0.938	-4.616	0.594	2.385	0.894	0.816	-0.069	-0.093	0.919	0.640	-1.597	-1.105	-9.592	Debye-Huckel
200	Inflow	2/12/15	0.629	-1.246	-4.504	0.464	2.268	1.040	0.954	-0.111	-0.110	0.903	0.625	-1.632	-1.415	-9.844	Debye-Huckel
200	Inflow	3/7/15	1.053	-1.042	-4.919	0.888	3.019	1.393	1.310	0.024	-0.103	0.910	0.631	-1.500	-1.212	-10.250	Debye-Huckel
200	Inflow	4/7/15	0.375	-1.241	-4.608	0.210	1.762	0.790	0.803	-0.002	-0.045	0.967	0.688	-1.621	-1.408	-9.955	Debye-Huckel
200	Inflow	5/5/15	1.719	-1.302	-4.720	1.555	4.460	2.109	2.011	-0.202	-0.066	0.947	0.669	-1.711	-1.472	-10.140	Debye-Huckel
200	Inflow	6/3/15	1.557	-1.306	-4.647	1.392	4.207	2.086	2.063	-0.005	-0.115	0.910	0.629	-1.599	-1.493	-10.040	Debye-Huckel
200	Inflow	7/13/15	0.693	-1.256	-4.653	0.528	2.393	1.124	1.037	-0.116	-0.068	0.957	0.676	-1.645	-1.442	-9.975	Debye-Huckel
200	Inflow	8/8/15	0.493	-1.187	-4.566	0.328	1.988	0.881	0.508	-0.366	-0.026	0.990	0.711	-1.602	-1.360	-9.866	Debye-Huckel
200	Inflow	9/6/15	0.977	-1.320	-4.588	0.812	2.959	1.378	1.358	-0.138	-0.087	0.933	0.653	-1.731	-1.500	-9.870	Debye-Huckel
200	Inflow	10/12/15	1.248	-1.274	-4.692	1.083	3.531	1.695	1.596	-0.121	-0.044	0.973	0.693	-1.632	-1.449	-10.040	Debye-Huckel
200	Inflow	11/10/15	1.268	-1.327	-4.603	1.103	3.573	1.698	1.464	-0.327	-0.081	0.937	0.657	-1.705	-1.504	-9.916	Debye-Huckel
200	Inflow	12/8/15	1.234	-1.054	-5.021	1.070	3.404	1.599	1.492	0.023	-0.069	0.935	0.658	-1.470	-1.211	-10.430	Debye-Huckel
200	Inflow	1/15/16	1.273	-1.184	-4.953	1.108	3.476	1.675	1.608	-0.046	-0.075	0.940	0.660	-1.590	-1.361	-10.320	Debye-Huckel
200	Inflow	2/16/16	1.091	-1.251	-4.941	0.926	3.129	1.497	1.322	-0.215	-0.005	1.012	0.732	-1.651	-1.426	-10.300	Debye-Huckel
200	Inflow	2/16/16	1.091	-1.251	-4.941	0.926	3.129	1.497	1.322	-0.215	-0.005	1.012	0.732	-1.651	-1.426	-10.300	Debye-Huckel
200	Inflow	2/16/16	1.102	-1.252	-4.942	0.938	3.156	1.497	1.313	-0.230	-0.013	0.998	0.720	-1.652	-1.419	-10.300	Debye-Huckel
200	Inflow	2/16/16	1.102	-1.252	-4.942	0.938	3.156	1.497	1.313	-0.230	-0.013	0.998	0.720	-1.652	-1.419	-10.300	Debye-Huckel
200	Inflow	3/9/16	1.131	-1.294	-4.941	0.967	2.976	1.483			-0.312	0.705	0.425	-1.748	-1.469	-10.330	Debye-Huckel
200	Inflow	5/5/16	0.386	-1.204	-4.830	0.221	1.743	0.884						-1.513	-1.381	-10.080	Debye-Huckel
200	Inflow	10/23/16	-0.197	-1.153	-3.232										-1.365		Harvie-Moller-Weare
200	Inflow	5/22/17	0.240	-0.942	-3.653										-1.157		Harvie-Moller-Weare
200	Inflow	8/21/17	0.292	-1.001	-3.929										-1.217		Harvie-Moller-Weare
200	Inflow	11/16/17	0.550	-0.797	-4.016										-1.013		Harvie-Moller-Weare
292	Inflow	8/1/16	0.475	-1.175	-4.788	0.310	1.900	1.384						-1.074	-1.353	-10.120	Debye-Huckel
292	Inflow	10/23/16	0.243	-1.207	-4.838	0.078	1.440	0.699						-1.559	-1.384	-10.180	Debye-Huckel
292	Inflow	12/17/16	0.437	-1.223	-4.830	0.272	1.837	0.905						-1.562	-1.400	-10.140	Debye-Huckel
292	Inflow	2/11/17	0.456	-1.237	-4.781	0.291	1.914	0.962						-1.548	-1.421	-10.110	Debye-Huckel
292	Inflow	5/24/17	0.660	-1.273	-4.884	0.495	2.265	1.109						-1.631	-1.450	-10.260	Debye-Huckel
292	Inflow	8/21/17	1.400	-1.179	-4.858	1.235	3.729	1.756						-1.631	-1.356	-10.170	Debye-Huckel
292	Inflow	11/19/17	1.086	-1.020	-5.045	0.921	3.107	1.428						-1.487	-1.198	-10.490	Debye-Huckel
204	TZ Shallow	10/22/13	0.495	-0.954	-3.724										-1.169		Harvie-Moller-Weare
204	TZ Shallow	11/22/13	0.864	-0.886	-3.720										-1.101		Harvie-Moller-Weare
204	TZ Shallow	12/19/13	0.368	-0.876	-3.900										-1.091		Harvie-Moller-Weare
204	TZ Shallow	1/17/14	0.450	-0.906	-3.762										-1.121		Harvie-Moller-Weare
204	TZ Shallow	2/16/14	0.494	-0.950	-4.035										-1.166		Harvie-Moller-Weare
204	TZ Shallow	3/19/14	0.275	-0.844	-3.928										-1.060		Harvie-Moller-Weare
204	TZ Shallow	4/16/14	0.277	-0.903	-3.850										-1.118		Harvie-Moller-Weare
204	TZ Shallow	5/18/14	0.280	-0.929	-3.901										-1.144		Harvie-Moller-Weare
204	TZ Shallow	6/12/14	0.291	-0.911	-3.873										-1.127		Harvie-Moller-Weare
204	TZ Shallow	7/19/14	0.303	-0.904	-3.935										-1.120		Harvie-Moller-Weare
204	TZ Shallow	8/16/14	0.289	-0.958	-3.905										-1.173		Harvie-Moller-Weare
204	TZ Shallow	10/11/14	0.313	-1.002	-3.970										-1.218		Harvie-Moller-Weare
204	TZ Shallow	11/4/14	0.388	-0.964	-4.029										-1.180		Harvie-Moller-Weare
204	TZ Shallow	12/4/14	0.850	-0.576	-3.840										-0.791		Harvie-Moller-Weare
204	TZ Shallow	1/9/15	0.360	-0.940	-4.087										-1.157		Harvie-Moller-Weare
204	TZ Shallow	2/11/15	0.548	-0.987	-4.019										-1.203		Harvie-Moller-Weare
204	TZ Shallow	3/5/15	0.564	-1.010	-3.976										-1.226		Harvie-Moller-Weare
204	TZ Shallow	5/5/15	1.166	-0.676	-3.660										-0.890		Harvie-Moller-Weare
204	TZ Shallow	6/7/15	0.621	-0.668	-3.563										-0.882		Harvie-Moller-Weare
204	TZ Shallow	7/13/15	0.459	-0.745	-3.566										-0.959		Harvie-Moller-Weare
204	TZ Shallow	8/5/15	0.686	-0.566	-3.539										-0.780		Harvie-Moller-Weare
204	TZ Shallow	9/2/15	0.603	-0.669	-3.625										-0.884		Harvie-Moller-Weare
204	TZ Shallow	10/7/15	0.839	-0.526	-3.442										-0.739		Harvie-Moller-Weare
204	TZ Shallow	11/5/15	1.021	-0.713	-3.573										-0.927		Harvie-Moller-Weare
204	TZ Shallow	12/9/15	1.187	-0.687	-3.549										-0.901		Harvie-Moller-Weare
204	TZ Shallow	1/13/16	0.749	-0.748	-3.496										-0.962		Harvie-Moller-Weare
204	TZ Shallow	2/15/16	0.859	-0.579	-3.529										-0.793		Harvie-Moller-Weare
205	TZ Shallow	10/22/13	0.347	-1.069	-3.135										-1.281		Harvie-Moller-Weare
205	TZ Shallow	11/22/13	0.572	-1.032	-3.138										-1.243		Harvie-Moller-Weare
205	TZ Shallow	12/19/13	0.552	-1.060	-3.194										-1.272		Harvie-Moller-Weare
205	TZ Shallow	1/16/14	0.311	-1.125	-3.000										-1.335		Harvie-Moller-Weare
205	TZ Shallow	2/17/14	0.535	-1.049	-3.175										-1.261		Harvie-Moller-Weare
205	TZ Shallow	3/20/14	0.156	-1.051	-3.181										-1.263		Harvie-Moller-Weare
205	TZ Shallow	4/16/14	0.317	-1.270	-3.194										-1.482		Harvie-Moller-Weare
205	TZ Shallow	5/18/14	0.169	-1.072	-3.259										-1.284		Harvie-Moller-Weare
205	TZ Shallow	6/12/14	0.186	-1.098	-3.265										-1.311		Harvie-Moller-Weare
205	TZ Shallow	7/17/14	0.489	-1.055	-3.253										-1.268		Harvie-Moller-Weare
205	TZ Shallow	8/16/14	0.085	-1.054	-3.130										-1.265		Harvie-Moller-Weare
205	TZ Shallow	10/11/14	0.333	-1.071	-3.143										-1.283		Harvie-Moller-Weare
205	TZ Shallow	11/4/14	0.324	-1.004	-3.263										-1.217		Harvie-Moller-Weare
205	TZ Shallow	12/4/14	0.297	-1.065	-3.300										-1.278		Harvie-Moller-Weare
205	TZ Shallow	1/9/15	0.379	-1.012	-3.354										-1.225		Harvie-Moller-Weare
205	TZ Shallow	2/10/15	0.371	-1.141	-3.263										-1.353		Harvie-Moller-Weare
205	TZ Shallow	5/6/15	1.189	-1.013	-3.326										-1.226		Harvie-Moller-Weare
205	TZ Shallow	6/2/15	1.359	-1.027	-3.256										-1.240		Harvie-Moller-Weare
205	TZ Shallow	7/14/15	0.393	-1.140	-3.288										-1.352		Harvie-Moller-Weare
205	TZ Shallow	8/5/15	0.600	-0.927	-3.299										-1.139		Harvie-Moller-Weare
205	TZ Shallow	9/2/15	0.722	-1.035	-3.294										-1.248		Harvie-Moller-Weare
205	TZ Shallow	10/7/15	0.915	-0.883	-3.261										-1.095		Harvie-Moller-Weare
205	TZ Shallow	11/4/15	0.900	-0.948	-3.418										-1.161		Harvie-Moller-Weare
205	TZ Shallow	12/2/15	1.118	-0.928	-3.402										-1.141		Harvie-Moller-Weare
205	TZ Shallow	1/12/16	0.798	-0.931	-3.296										-1.144		Harvie-Moller-Weare
205	TZ Shallow	2/15/16	0.839	-1.070	-3.244										-1.282		Harvie-Moller-Weare
205	TZ Shallow	3/10/16	1.127	-1.083	-3.335										-1.296		Harvie-Moller-Weare
205	TZ Shallow	5/18/16	0.198	-0.952	-3.448										-1.166		Harvie-Moller-Weare
205	TZ Shallow	10/11/16	0.035	-1.033	-3.251										-1.246		Harvie-Moller-Weare
205	TZ Shallow	12/16/16	0.310	-1.045	-3.304										-1.258		Harvie-Moller-Weare

205	TZ Shallow	2/10/17	0.120	-1.057	-3.346										-1.270		Harvie-Moller-Weare
205	TZ Shallow	5/22/17	0.132	-1.041	-3.310										-1.254		Harvie-Moller-Weare
205	TZ Shallow	8/22/17	0.667	-0.893	-3.280										-1.106		Harvie-Moller-Weare
205	TZ Shallow	11/18/17	0.312	-0.900	-3.299										-1.113		Harvie-Moller-Weare
206	TZ Shallow	11/22/13	0.731	-1.385	-4.200	0.566	2.756	1.765			-0.174	0.857	0.575	-1.182	-1.580	-9.778	Debye-Huckel
206	TZ Shallow	12/19/13	0.296	-1.386	-4.417	0.130	2.119	1.456			0.607	1.654	1.369	-1.088	-1.604	-9.774	Debye-Huckel
206	TZ Shallow	1/16/14	0.777	-1.411	-4.227	0.613	2.863	0.811	3.679	2.357	-0.593	0.373	0.103	-2.080	-1.509	-9.833	Debye-Huckel
206	TZ Shallow	2/16/14	0.427	-1.379	-4.343	0.262	2.057	1.737			-0.166	0.906	0.616	-0.977	-1.631	-9.810	Debye-Huckel
206	TZ Shallow	3/19/14	0.556	-1.123	-4.227	0.391	2.079	1.049	0.930	0.003	0.012	1.077	0.788	-1.526	-1.366	-9.331	Debye-Huckel
206	TZ Shallow	4/16/14	0.397	-1.308	-4.289	0.231	1.943	1.111	1.064	0.091	0.031	1.116	0.823	-1.525	-1.578	-9.654	Debye-Huckel
206	TZ Shallow	5/18/14	0.441	-1.337	-4.242	0.275	2.028	1.137	1.093	0.047	-0.040	1.046	0.753	-1.574	-1.608	-9.661	Debye-Huckel
206	TZ Shallow	6/12/14	0.269	-1.358	-4.286	0.103	1.653	0.999	0.922	0.019	-0.039	1.054	0.760	-1.574	-1.638	-9.711	Debye-Huckel
206	TZ Shallow	7/17/14	0.512	-1.408	-4.276	0.346	2.138	1.210	1.134	-0.046	-0.067	1.011	0.720	-1.627	-1.668	-9.659	Debye-Huckel
206	TZ Shallow	8/16/14	0.316	-1.350	-4.243	0.150	1.779	1.076	0.996	0.056	-0.048	1.044	0.750	-1.534	-1.629	-9.666	Debye-Huckel
206	TZ Shallow	10/11/14	0.883	-1.093	-4.176	0.717	2.628	1.329	1.229	-0.017	-0.095	0.992	0.699	-1.582	-1.366	-9.329	Debye-Huckel
206	TZ Shallow	11/4/14	0.504	-1.326	-4.282	0.338	2.161	1.246	1.198	0.095	-0.059	1.030	0.737	-1.524	-1.602	-9.722	Debye-Huckel
206	TZ Shallow	12/4/14	0.586	-1.317	-4.329	0.421	2.312	1.292	1.219	0.049	-0.045	1.039	0.747	-1.541	-1.585	-9.748	Debye-Huckel
206	TZ Shallow	1/9/15	0.564	-1.320	-4.300	0.398	2.282	1.275	1.203	0.057	-0.071	1.009	0.718	-1.532	-1.584	-9.740	Debye-Huckel
206	TZ Shallow	2/11/15	0.651	-1.326	-4.316	0.485	2.412	1.367	1.297	0.052	-0.069	1.015	0.723	-1.541	-1.596	-9.711	Debye-Huckel
206	TZ Shallow	3/5/15	0.872	-1.320	-4.249	0.706	2.898	1.607	1.540	0.077	-0.046	1.042	0.749	-1.522	-1.594	-9.642	Debye-Huckel
206	TZ Shallow	5/5/15	1.345	-1.253	-4.300	1.179	3.771	2.012	1.915	0.041	-0.049	1.044	0.750	-1.531	-1.533	-9.658	Debye-Huckel
206	TZ Shallow	6/3/15	1.445	-1.327	-4.281	1.279	4.011	2.207	2.204	0.149	-0.139	0.960	0.665	-1.523	-1.617	-9.718	Debye-Huckel
206	TZ Shallow	7/15/15	0.670	-1.300	-4.365	0.504	2.481	1.356	1.275	0.025	-0.078	1.019	0.725	-1.568	-1.587	-9.686	Debye-Huckel
206	TZ Shallow	8/5/15	0.693	-1.268	-4.274	0.527	2.505	1.422	1.507	0.271	-0.033	1.059	0.765	-1.483	-1.547	-9.667	Debye-Huckel
206	TZ Shallow	9/2/15	0.908	-1.322	-4.372	0.742	2.939	1.633	1.588	0.084	-0.064	1.026	0.733	-1.539	-1.599	-9.852	Debye-Huckel
206	TZ Shallow	10/7/15	1.186	-1.153	-4.278	1.020	3.522	1.908	1.895	0.289	-0.003	1.082	0.790	-1.362	-1.423	-9.711	Debye-Huckel
206	TZ Shallow	10/7/15	1.186	-1.153	-4.278	1.020	3.522	1.908	1.895	0.289	-0.003	1.082	0.790	-1.362	-1.423	-9.711	Debye-Huckel
206	TZ Shallow	10/7/15	1.171	-1.151	-4.275	1.005	3.486	1.909	1.907	0.311	0.008	1.101	0.807	-1.358	-1.431	-9.707	Debye-Huckel
206	TZ Shallow	10/7/15	1.171	-1.151	-4.275	1.005	3.486	1.909	1.907	0.311	0.008	1.101	0.807	-1.358	-1.431	-9.707	Debye-Huckel
206	TZ Shallow	11/5/15	1.141	-1.285	-4.272	0.975	3.425	1.886	1.721	0.022	0.017	1.107	0.814	-1.481	-1.562	-9.705	Debye-Huckel
206	TZ Shallow	12/2/15	0.844	-1.329	-4.295	0.678	2.805	1.554	1.549	0.109	0.028	1.113	0.821	-1.550	-1.599	-9.699	Debye-Huckel
206	TZ Shallow	1/12/16	0.984	-1.256	-4.256	0.819	3.136	1.704	1.325	-0.179	-0.049	1.032	0.740	-1.459	-1.520	-9.698	Debye-Huckel
206	TZ Shallow	2/15/16	0.971	-1.310	-4.246	0.805	3.083	1.697	1.419	-0.138	0.084	1.177	0.883	-1.531	-1.591	-9.674	Debye-Huckel
206	TZ Shallow	2/15/16	0.971	-1.310	-4.246	0.805	3.083	1.697	1.419	-0.138	0.084	1.177	0.883	-1.531	-1.591	-9.674	Debye-Huckel
206	TZ Shallow	2/15/16	0.996	-1.313	-4.252	0.830	3.143	1.696	1.399	-0.173	0.066	1.146	0.855	-1.537	-1.577	-9.681	Debye-Huckel
206	TZ Shallow	2/15/16	0.996	-1.313	-4.252	0.830	3.143	1.696	1.399	-0.173	0.066	1.146	0.855	-1.537	-1.577	-9.681	Debye-Huckel
206	TZ Shallow	3/9/16	1.029	-1.227	-4.214	0.863	3.228	1.625	1.361	-0.169	0.380	1.471	1.177	-1.573	-1.505	-9.704	Debye-Huckel
206	TZ Shallow	5/19/16	0.461	-1.268	-4.304	0.296	2.074	1.150						-1.386	-1.445	-9.680	Debye-Huckel
206	TZ Shallow	10/10/16	0.417	-1.301	-4.171	0.252	2.055	0.994						-1.530	-1.477	-9.583	Debye-Huckel
206	TZ Shallow	12/16/16	0.670	-1.317	-4.256	0.505	2.565	1.266						-1.527	-1.493	-9.676	Debye-Huckel
206	TZ Shallow	2/10/17	0.644	-1.301	-4.192	0.479	2.496	1.393						-1.461	-1.554	-9.621	Debye-Huckel
206	TZ Shallow	5/22/17	0.799	-1.286	-4.291	0.634	2.768	1.338						-1.554	-1.463	-9.669	Debye-Huckel
206	TZ Shallow	8/22/17	0.729	-1.239	-4.242	0.565	2.656	1.326						-1.449	-1.415	-9.594	Debye-Huckel
206	TZ Shallow	11/18/17		-1.331	-3.785										-1.546		Harvie-Moller-Weare
35	Lagoon	1/1/98	1.468	-0.587	-0.987										-0.708		Harvie-Moller-Weare
35	Lagoon	4/1/98	1.530	-0.505	-1.470										-0.666		Harvie-Moller-Weare
35	Lagoon	4/1/99	1.327	-0.345	-1.488										-0.507		Harvie-Moller-Weare
35	Lagoon	10/1/99	1.305	-0.882	-1.918										-1.067		Harvie-Moller-Weare
35	Lagoon	1/1/00	1.490	-0.399	-1.248										-0.545		Harvie-Moller-Weare
35	Lagoon	4/1/00	1.337	-0.487	-1.502										-0.652		Harvie-Moller-Weare
35	Lagoon	7/1/00	0.811	-1.046	-2.057										-1.237		Harvie-Moller-Weare
35	Lagoon	10/1/00	1.592	-0.486	-1.787										-0.665		Harvie-Moller-Weare
35	Lagoon	1/1/01	1.788	-0.382	-1.212										-0.525		Harvie-Moller-Weare
35	Lagoon	4/1/01	1.540	-0.301	-1.143										-0.438		Harvie-Moller-Weare
35	Lagoon	10/1/01	1.538	-0.373	-1.320										-0.524		Harvie-Moller-Weare
35	Lagoon	7/1/02	1.412	-0.675	-1.973										-0.862		Harvie-Moller-Weare
35	Lagoon	10/1/02	1.555	-0.427	-1.496										-0.590		Harvie-Moller-Weare
35	Lagoon	1/1/03	1.289	-0.382	-0.997										-0.503		Harvie-Moller-Weare
35	Lagoon	4/1/03	1.425	-0.478	-0.999										-0.601		Harvie-Moller-Weare
35	Lagoon	7/1/03	1.333	-0.723	-1.964										-0.910		Harvie-Moller-Weare
35	Lagoon	10/1/03	1.192	-1.153	-1.475										-1.317		Harvie-Moller-Weare
35	Lagoon	1/1/04	1.463	0.067	-1.141										-0.067		Harvie-Moller-Weare
35	Lagoon	4/1/04	1.418	0.078	-1.383										-0.076		Harvie-Moller-Weare
35	Lagoon	7/1/04	0.590	-0.386	-2.162										-0.579		Harvie-Moller-Weare
35	Lagoon	10/1/04	0.052	-0.432	-1.958										-0.618		Harvie-Moller-Weare
35	Lagoon	1/1/05	1.058	-0.164	-1.305										-0.312		Harvie-Moller-Weare
35	Lagoon	5/5/05	1.099	-0.349	-1.823										-0.529		Harvie-Moller-Weare
35	Lagoon	10/5/05	1.602	0.127	-1.768										-0.051		Harvie-Moller-Weare
35	Lagoon	1/1/06	-0.392	-0.322	-1.412										-0.479		Harvie-Moller-Weare
35	Lagoon	4/1/06	0.661	-0.136	-1.481										-0.298		Harvie-Moller-Weare
35	Lagoon	10/1/06	0.866	-0.276	-1.789										-0.455		Harvie-Moller-Weare
35	Lagoon	1/1/07	0.303	0.016	-1.231										-0.127		Harvie-Moller-Weare
35	Lagoon	4/1/07	0.369	-0.315	-1.538										-0.481		Harvie-Moller-Weare
35	Lagoon	7/1/07		-0.343	-2.265										-0.539		Harvie-Moller-Weare
35	Lagoon	1/1/08	1.143	0.228	-1.572										0.063		Harvie-Moller-Weare
35	Lagoon	7/1/08	1.129	-0.441	-2.156										-0.634		Harvie-Moller-Weare
35	Lagoon	10/1/08	0.694	-0.357	-1.777										-0.535		Harvie-Moller-Weare
35	Lagoon	1/1/09	0.354	-0.498	-1.386										-0.653		Harvie-Moller-Weare
35	Lagoon	4/1/09	0.776	-0.350	-1.749										-0.527		Harvie-Moller-Weare
35	Lagoon	7/1/09	0.849	-0.685	-2.201										-0.880		Harvie-Moller-Weare
35	Lagoon	10/1/09	0.683	-0.422	-2.069										-0.612		Harvie-Moller-Weare
35	Lagoon	1/1/10		-0.122	-1.359										-0.275		Harvie-Moller-Weare
35	Lagoon	7/1/10	1.257	-0.377	-2.280										-0.573		Harvie-Moller-Weare
35	Lagoon	10/1/10	1.002	-0.276	-1.854										-0.458		Harvie-Moller-Weare
35	Lagoon	1/1/11	0.674	0.081	-1.410										-0.074		Harvie-Moller-Weare
35	Lagoon	4/1/11	1.175	-0.026	-1.729										-0.202		Harvie-Moller-Weare
35	Lagoon	7/1/11	0.956	-0.386	-2.218										-0.581		Harvie-Moller-Weare
35	Lagoon	10/1/11	1.363	0.038	-1.821										-0.142		Harvie-Moller-Weare
35	Lagoon	1/1/12	0.626	-0.111	-1.475										-0.272		Harvie-Moller-Weare
35	Lagoon	4/1/12	0.788	-0.239	-1.992										-0.427		Harvie-Moller-Weare
35	Lagoon	7/1/12	0.930	-0.162	-2.321										-0.359		Harvie-Moller-Weare
35	Lagoon	1/1/13	0.610	0.092	-1.360										-0.060		Harvie-Moller-Weare
35	Lagoon	4/1/13	1.371	0.020	-1.827										-0.160		Harvie-Moller-Weare
35	Lagoon	10/1/13	0.837	-0.310	-1.945										-0.496		Harvie-Moller-Weare
36	Lagoon	4/1/98	1.515	-0.612	-1.582										-0.779		Harvie-Moller-Weare
36	Lagoon	7/1/98	1.282	-1.039	-2.083										-1.230		Harvie-Moller-Weare
36	Lagoon	4/1/99	1.210	-0.771	-1.546										-0.938		Harvie-Moller-Weare
36	Lagoon	7/1/99	1.450	-0.837	-2.123										-1.030		Harvie-Moller-Weare
36	Lagoon	10/1/99	1.200	-1.111	-2.096										-1.303		Harvie-Moller-Weare
36	Lagoon	1/1/00	1.441	-0.638	-1.498										-0.802		Harvie-Moller-Weare
36	Lagoon	4/1/00	1.120	-0.709	-1.589										-0.879		Harvie-Moller-Weare
36	Lagoon	7/1/00	0.788	-1.332	-2.133										-1.526		Harvie-Moller-Weare
36	Lagoon	10/1/00	1.326	-0.823	-1.998										-1.012		Harvie-Moller-Weare
36	Lagoon	4/1/01	1.450	-0.458	-1.345										-0.613		Harvie-Moller-Weare
36	Lagoon	7/1/01	1.130	-0.895	-1.746										-1.074		Harvie-Moller-Weare
36	Lagoon	10/1/01	1.221	-0.825	-1.669										-0.999		Harvie-Moller-Weare
36	Lagoon	1/1/02	1.297	-0.464	-1.274										-0.612		Harvie-Moller-Weare
36	Lagoon	7/1/02	1.037	-0.845	-1.954										-1.032		Harvie-Moller-Weare
36	Lagoon	10/1/02	1.338	-0.754	-1.769										-0.933		Harvie-Moller-Weare
36	Lagoon	1/1/03	1.303	-0.602	-1.434										-0.760		Harvie-Moller-Weare
36	Lagoon	4/1/03	1.165	-0.907	-1.557										-1.074		Harvie-Moller-Weare
36	Lagoon	7/1/03	1.115	-1.012	-1.977										-1.200		Harvie-Moller-Weare
36	Lagoon	10/1/03	1.170	-1.101	-1.710										-1.278		Harvie-Moller-Weare

36	Lagoon	1/1/04	1.436	-1.004	-1.456	-1.165	Harvie-Moller-Weare
36	Lagoon	4/1/04	1.349	-0.113	-1.487	-0.275	Harvie-Moller-Weare
36	Lagoon	10/1/04	0.719	-1.411	-1.997	-1.599	Harvie-Moller-Weare
36	Lagoon	1/1/05	1.062	-0.641	-1.455	-0.802	Harvie-Moller-Weare
36	Lagoon	5/5/05	1.230	-0.283	-1.903	-0.466	Harvie-Moller-Weare
36	Lagoon	10/5/05	1.688	-0.169	-1.921	-0.355	Harvie-Moller-Weare
36	Lagoon	1/1/06	0.242	-0.387	-1.571	-0.555	Harvie-Moller-Weare
36	Lagoon	4/1/06	0.543	-0.270	-1.662	-0.443	Harvie-Moller-Weare
36	Lagoon	10/1/06	1.003	-0.393	-1.953	-0.580	Harvie-Moller-Weare
36	Lagoon	1/1/07	0.783	-0.513	-1.826	-0.694	Harvie-Moller-Weare
36	Lagoon	4/1/07	0.892	-0.586	-1.900	-0.770	Harvie-Moller-Weare
36	Lagoon	7/1/07	0.981	-0.524	-2.249	-0.720	Harvie-Moller-Weare
36	Lagoon	11/1/07	0.988	-0.424	-2.087	-0.615	Harvie-Moller-Weare
36	Lagoon	1/1/08	0.982	-1.243	-1.921	-1.427	Harvie-Moller-Weare
36	Lagoon	4/1/08	0.896	-0.469	-1.957	-0.655	Harvie-Moller-Weare
36	Lagoon	7/1/08	1.136	-0.513	-2.210	-0.708	Harvie-Moller-Weare
36	Lagoon	10/1/08	0.927	-0.558	-1.977	-0.745	Harvie-Moller-Weare
36	Lagoon	1/1/09	0.537		-1.565		Harvie-Moller-Weare
36	Lagoon	4/1/09	0.589		-1.724		Harvie-Moller-Weare
36	Lagoon	7/1/09	0.801		-2.195		Harvie-Moller-Weare
36	Lagoon	10/1/09	1.294		-1.928		Harvie-Moller-Weare
36	Lagoon	1/1/10	0.813	-0.516	-1.745	-0.694	Harvie-Moller-Weare
36	Lagoon	4/1/10	1.284	-0.272	-1.985	-0.460	Harvie-Moller-Weare
36	Lagoon	10/1/10	1.040	-0.433	-2.022	-0.621	Harvie-Moller-Weare
36	Lagoon	4/1/11	1.051	-0.191	-1.931	-0.375	Harvie-Moller-Weare
36	Lagoon	7/1/11	0.978	-0.457	-2.328	-0.655	Harvie-Moller-Weare
36	Lagoon	10/1/11	1.559	-0.214	-2.019	-0.402	Harvie-Moller-Weare
36	Lagoon	1/1/12	0.921	-0.228	-1.556	-0.393	Harvie-Moller-Weare
36	Lagoon	4/1/12	0.912	-0.588	-1.955	-0.775	Harvie-Moller-Weare
36	Lagoon	7/1/12	0.941	-0.425	-2.286	-0.622	Harvie-Moller-Weare
36	Lagoon	10/1/12	1.066	-0.398	-2.061	-0.588	Harvie-Moller-Weare
36	Lagoon	5/17/13	0.800	-0.755	-3.218	-0.966	Harvie-Moller-Weare
36	Lagoon	6/20/13	1.293	-0.418	-2.508	-0.620	Harvie-Moller-Weare
36	Lagoon	7/1/13	0.975	-0.378	-2.247	-0.573	Harvie-Moller-Weare
36	Lagoon	8/18/13	1.222	-0.609	-2.227	-0.805	Harvie-Moller-Weare
36	Lagoon	9/3/13	1.514	-0.543	-2.066	-0.734	Harvie-Moller-Weare
36	Lagoon	10/1/13	0.941	-0.377	-2.028	-0.566	Harvie-Moller-Weare
36	Lagoon	12/12/13	1.921	-0.147	-1.657	-0.320	Harvie-Moller-Weare
36	Lagoon	1/18/14	1.632	-0.241	-1.500	-0.404	Harvie-Moller-Weare
36	Lagoon	2/16/14	2.085	-0.333	-1.490	-0.496	Harvie-Moller-Weare
36	Lagoon	4/18/14	1.208	-0.320	-1.659	-0.493	Harvie-Moller-Weare
36	Lagoon	5/17/14	0.990	-0.415	-1.892	-0.599	Harvie-Moller-Weare
36	Lagoon	6/10/14	1.191	-0.418	-2.059	-0.608	Harvie-Moller-Weare
36	Lagoon	7/17/14	1.167	-0.496	-2.137	-0.689	Harvie-Moller-Weare
36	Lagoon	8/12/14	0.965	-0.610	-2.207	-0.805	Harvie-Moller-Weare
36	Lagoon	9/7/14	1.319	-0.615	-2.177	-0.809	Harvie-Moller-Weare
36	Lagoon	10/7/14	1.335	-0.445	-2.004	-0.633	Harvie-Moller-Weare
36	Lagoon	11/5/14	1.396	-0.511	-2.039	-0.700	Harvie-Moller-Weare
36	Lagoon	12/3/14	1.335	-0.243	-1.781	-0.421	Harvie-Moller-Weare
36	Lagoon	1/6/15	1.419	-0.363	-1.736	-0.540	Harvie-Moller-Weare
36	Lagoon	2/11/15	1.666	-0.362	-1.714	-0.538	Harvie-Moller-Weare
36	Lagoon	3/4/15	1.579	-0.275	-1.577	-0.442	Harvie-Moller-Weare
36	Lagoon	5/5/15	1.376	-0.177	-1.767	-0.355	Harvie-Moller-Weare
36	Lagoon	6/3/15	1.414	-0.345	-2.033	-0.534	Harvie-Moller-Weare
36	Lagoon	7/9/15	1.263	-0.359	-2.198	-0.553	Harvie-Moller-Weare
36	Lagoon	8/5/15	1.198	-0.402	-2.170	-0.596	Harvie-Moller-Weare
36	Lagoon	9/1/15	1.142	-0.449	-2.066	-0.640	Harvie-Moller-Weare
36	Lagoon	10/8/15	1.341	-0.252	-1.804	-0.432	Harvie-Moller-Weare
36	Lagoon	11/4/15	1.386	-0.227	-1.828	-0.408	Harvie-Moller-Weare
36	Lagoon	12/2/15	1.427	-0.180	-1.605	-0.349	Harvie-Moller-Weare
36	Lagoon	1/12/16	1.378	-0.118	-1.409	-0.274	Harvie-Moller-Weare
36	Lagoon	2/17/16	1.422	-0.212	-1.543	-0.377	Harvie-Moller-Weare
36	Lagoon	3/10/16	1.422	-0.227	-1.319	-0.377	Harvie-Moller-Weare
37	Lagoon	4/1/98	0.880	-0.645	-3.028	-0.855	Harvie-Moller-Weare
37	Lagoon	4/1/99	0.725	-0.978	-3.219	-1.190	Harvie-Moller-Weare
37	Lagoon	1/1/00	0.692	-1.528	-3.193	-1.740	Harvie-Moller-Weare
37	Lagoon	4/1/00	0.619	-1.304	-3.146	-1.516	Harvie-Moller-Weare
37	Lagoon	7/1/00	0.669	-1.399	-2.878	-1.608	Harvie-Moller-Weare
37	Lagoon	1/1/01	0.754	-1.244	-3.170	-1.455	Harvie-Moller-Weare
37	Lagoon	7/1/01	0.907	-0.944	-2.690	-1.149	Harvie-Moller-Weare
37	Lagoon	10/1/01	0.721	-1.112	-2.770	-1.320	Harvie-Moller-Weare
37	Lagoon	1/1/02	0.629	-1.131	-2.950	-1.341	Harvie-Moller-Weare
37	Lagoon	7/1/02	0.934	-0.877	-2.627	-1.082	Harvie-Moller-Weare
37	Lagoon	10/1/02	1.171	-1.199	-3.007	-1.409	Harvie-Moller-Weare
37	Lagoon	1/1/03	0.782	-1.186	-2.975	-1.396	Harvie-Moller-Weare
37	Lagoon	4/1/03	0.907	-1.158	-2.951	-1.367	Harvie-Moller-Weare
37	Lagoon	7/1/03	1.020	-1.042	-2.811	-1.250	Harvie-Moller-Weare
37	Lagoon	10/1/03	0.674	-1.344	-2.846	-1.552	Harvie-Moller-Weare
37	Lagoon	1/1/04	0.776	-0.874	-3.094	-1.085	Harvie-Moller-Weare
37	Lagoon	4/1/04	0.856	-0.679	-3.071	-0.890	Harvie-Moller-Weare
37	Lagoon	7/1/04	0.444	-0.574	-2.243	-0.769	Harvie-Moller-Weare
37	Lagoon	10/1/04	0.410	-0.929	-3.135	-1.140	Harvie-Moller-Weare
37	Lagoon	1/1/05	0.607	-0.874	-3.026	-1.084	Harvie-Moller-Weare
37	Lagoon	5/5/05	0.386	-1.027	-3.074	-1.237	Harvie-Moller-Weare
37	Lagoon	7/5/05	0.876	-0.655	-3.140	-0.866	Harvie-Moller-Weare
37	Lagoon	10/5/05	1.239	-0.350	-3.145	-0.561	Harvie-Moller-Weare
37	Lagoon	1/1/06	0.355	-0.982	-3.110	-1.192	Harvie-Moller-Weare
37	Lagoon	4/1/06	0.632	-0.797	-3.215	-1.009	Harvie-Moller-Weare
37	Lagoon	7/1/06	0.739	-0.621	-3.161	-0.832	Harvie-Moller-Weare
37	Lagoon	10/1/06	0.777	-0.757	-3.132	-0.968	Harvie-Moller-Weare
37	Lagoon	1/1/07	0.808	-0.675	-3.207	-0.886	Harvie-Moller-Weare
37	Lagoon	4/1/07	0.666	-0.736	-3.001	-0.946	Harvie-Moller-Weare
37	Lagoon	7/1/07	0.802	-0.539	-3.045	-0.749	Harvie-Moller-Weare
37	Lagoon	11/1/07	0.688	-0.845	-3.187	-1.057	Harvie-Moller-Weare
37	Lagoon	1/1/08	0.938	-0.637	-3.341	-0.849	Harvie-Moller-Weare
37	Lagoon	4/1/08	0.720	-0.767	-3.186	-0.978	Harvie-Moller-Weare
37	Lagoon	7/1/08	0.867	-0.484	-2.838	-0.692	Harvie-Moller-Weare
37	Lagoon	10/1/08	0.483	-0.819	-3.283	-1.031	Harvie-Moller-Weare
37	Lagoon	1/1/09	0.824	-1.455	-3.177	-1.667	Harvie-Moller-Weare
37	Lagoon	4/1/09	0.914	-1.417	-3.214	-1.629	Harvie-Moller-Weare
37	Lagoon	10/1/09	0.794	-1.534	-3.336	-1.747	Harvie-Moller-Weare
37	Lagoon	1/1/10	0.597	-0.807	-3.273	-1.019	Harvie-Moller-Weare
37	Lagoon	7/1/10	0.967	-0.633	-3.098	-0.844	Harvie-Moller-Weare
37	Lagoon	10/1/10	0.776	-0.774	-3.313	-0.986	Harvie-Moller-Weare
37	Lagoon	7/1/11	0.809	-0.612	-2.842	-0.820	Harvie-Moller-Weare
37	Lagoon	10/1/11	0.773	-0.680	-3.251	-0.892	Harvie-Moller-Weare
37	Lagoon	1/1/12	0.477	-0.829	-3.215	-1.041	Harvie-Moller-Weare
37	Lagoon	4/1/12	0.786	-0.641	-2.780	-0.847	Harvie-Moller-Weare
37	Lagoon	7/1/12	0.769	-0.342	-2.936	-0.551	Harvie-Moller-Weare
37	Lagoon	10/1/12	0.861	-0.761	-3.433	-0.974	Harvie-Moller-Weare
37	Lagoon	1/1/13	0.667	-0.926	-3.210	-1.138	Harvie-Moller-Weare
37	Lagoon	2/14/13	0.825	-0.718	-3.177	-0.929	Harvie-Moller-Weare
37	Lagoon	4/1/13	1.163	-0.609	-3.199	-0.821	Harvie-Moller-Weare

37	Lagoon	4/21/13	0.946	-0.819	-3.095	-1.029	Harvie-Moller-Weare
37	Lagoon	7/25/13	0.703	-0.680	-2.865	-0.888	Harvie-Moller-Weare
37	Lagoon	8/14/13	0.692	-0.696	-2.845	-0.904	Harvie-Moller-Weare
37	Lagoon	9/3/13	0.866	-0.778	-2.937	-0.987	Harvie-Moller-Weare
37	Lagoon	10/1/13	0.742	-0.747	-3.263	-0.959	Harvie-Moller-Weare
37	Lagoon	10/16/13	0.796	-0.837	-3.193	-1.048	Harvie-Moller-Weare
37	Lagoon	11/23/13	1.220	-0.879	-3.182	-1.091	Harvie-Moller-Weare
37	Lagoon	12/17/13	1.151	-0.872	-3.176	-1.083	Harvie-Moller-Weare
37	Lagoon	1/18/14	0.974	-0.765	-3.136	-0.976	Harvie-Moller-Weare
37	Lagoon	2/16/14	1.318	-0.931	-3.192	-1.142	Harvie-Moller-Weare
37	Lagoon	4/18/14	0.650	-0.855	-3.152	-1.066	Harvie-Moller-Weare
37	Lagoon	5/17/14	0.348	-0.834	-3.138	-1.046	Harvie-Moller-Weare
37	Lagoon	6/10/14	0.802	-0.738	-3.073	-0.948	Harvie-Moller-Weare
37	Lagoon	7/17/14	0.677	-0.684	-3.020	-0.893	Harvie-Moller-Weare
37	Lagoon	10/7/14	0.869	-0.842	-3.322	-1.055	Harvie-Moller-Weare
37	Lagoon	11/5/14	0.804	-0.865	-3.349	-1.077	Harvie-Moller-Weare
37	Lagoon	12/3/14	0.832	-0.891	-3.256	-1.103	Harvie-Moller-Weare
37	Lagoon	1/6/15	0.739	-0.823	-3.056	-1.034	Harvie-Moller-Weare
37	Lagoon	2/11/15	1.008	-0.894	-3.139	-1.105	Harvie-Moller-Weare
37	Lagoon	3/4/15	0.909	-0.865	-3.245	-1.077	Harvie-Moller-Weare
37	Lagoon	5/5/15	1.075	-0.440	-2.586	-0.643	Harvie-Moller-Weare
37	Lagoon	6/3/15	1.070	-0.631	-2.754	-0.838	Harvie-Moller-Weare
37	Lagoon	7/13/15	0.825	-0.565	-2.893	-0.774	Harvie-Moller-Weare
37	Lagoon	8/5/15	0.820	-0.632	-2.823	-0.840	Harvie-Moller-Weare
37	Lagoon	9/1/15	0.689	-0.805	-2.969	-1.015	Harvie-Moller-Weare
37	Lagoon	10/8/15	0.827	-0.650	-2.959	-0.859	Harvie-Moller-Weare
37	Lagoon	11/4/15	0.836	-0.755	-3.118	-0.966	Harvie-Moller-Weare
37	Lagoon	12/2/15	0.981	-0.792	-3.092	-1.002	Harvie-Moller-Weare
37	Lagoon	1/12/16	0.813	-0.726	-3.097	-0.936	Harvie-Moller-Weare
37	Lagoon	2/17/16	1.180	-0.103	-2.161	-0.296	Harvie-Moller-Weare
37	Lagoon	3/10/16	0.900	-0.667	-3.075	-0.877	Harvie-Moller-Weare
28	Nucleus	3/22/13	0.093	-0.074	-0.403	-0.099	Harvie-Moller-Weare
28	Nucleus	6/12/13	0.614	0.019	-0.169	0.042	Harvie-Moller-Weare
28	Nucleus	7/20/13	0.385	-0.060	-0.003	-0.011	Harvie-Moller-Weare
28	Nucleus	8/17/13	1.475	-0.172	0.040	-0.113	Harvie-Moller-Weare
28	Nucleus	9/6/13	0.691	0.001	0.151	0.082	Harvie-Moller-Weare
28	Nucleus	10/17/13	0.640	-0.097	0.030	-0.044	Harvie-Moller-Weare
28	Nucleus	11/21/13	1.139	-0.129	0.112	-0.056	Harvie-Moller-Weare
28	Nucleus	12/10/13	1.350	-0.034	-0.082	-0.018	Harvie-Moller-Weare
203	Nucleus	9/6/13	0.672	-0.113	-0.156	-0.115	Harvie-Moller-Weare
112	ucleus Marg	2/19/13	0.716	-0.072	-0.050	-0.048	Harvie-Moller-Weare
113	ucleus Marg	2/19/13	0.765	-0.067	-0.049	-0.039	Harvie-Moller-Weare
202	ucleus Marg	7/20/13	0.960	-0.072	-0.025	-0.041	Harvie-Moller-Weare
202	ucleus Marg	8/18/13	1.197	-0.065	-0.067	-0.042	Harvie-Moller-Weare
202	ucleus Marg	9/6/13	1.157	-0.022	0.191	0.059	Harvie-Moller-Weare
202	ucleus Marg	10/18/13	1.176	-0.004	0.051	0.047	Harvie-Moller-Weare
202	ucleus Marg	11/20/13	1.957	-0.123	0.140	-0.053	Harvie-Moller-Weare
202	ucleus Marg	12/11/13	1.658	-0.177	0.074	-0.120	Harvie-Moller-Weare
202	ucleus Marg	1/17/14	0.989	-0.027	0.110	0.037	Harvie-Moller-Weare
202	ucleus Marg	2/14/14	1.561	-0.189	0.080	-0.130	Harvie-Moller-Weare
202	ucleus Marg	3/25/14	1.011	0.208	-0.134	0.220	Harvie-Moller-Weare
202	ucleus Marg	4/20/14	0.976	0.072	-0.011	0.118	Harvie-Moller-Weare
202	ucleus Marg	5/15/14	0.891	0.010	-0.105	0.033	Harvie-Moller-Weare
202	ucleus Marg	6/12/14	0.827	-0.103	-0.068	-0.077	Harvie-Moller-Weare
202	ucleus Marg	7/16/14	0.998	0.005	-0.008	0.048	Harvie-Moller-Weare
202	ucleus Marg	12/2/14	0.872	-0.069	-0.199	-0.069	Harvie-Moller-Weare
202	ucleus Marg	1/11/15	0.907	0.069	-0.198	0.071	Harvie-Moller-Weare
202	ucleus Marg	2/13/15	1.142	-0.029	-0.239	-0.035	Harvie-Moller-Weare
202	ucleus Marg	3/3/15	1.116	0.034	-0.061	0.061	Harvie-Moller-Weare
202	ucleus Marg	4/11/15	1.275	0.106	-0.036	0.143	Harvie-Moller-Weare
202	ucleus Marg	5/7/15	1.051	-0.076	-0.238	-0.085	Harvie-Moller-Weare
202	ucleus Marg	6/10/15	0.986	-0.016	-0.304	-0.035	Harvie-Moller-Weare
202	ucleus Marg	7/10/15	1.177	0.105	-0.330	0.085	Harvie-Moller-Weare
202	ucleus Marg	8/10/15	0.718	-0.107	-0.285	-0.123	Harvie-Moller-Weare
202	ucleus Marg	9/3/15	0.758	-0.195	-0.389	-0.226	Harvie-Moller-Weare
202	ucleus Marg	10/11/15	0.809	-0.170	-0.315	-0.190	Harvie-Moller-Weare
202	ucleus Marg	11/7/15	0.913	0.062	-0.016	0.105	Harvie-Moller-Weare
202	ucleus Marg	12/3/15	1.042	0.085	-0.079	0.111	Harvie-Moller-Weare
202	ucleus Marg	1/20/16	1.100	0.164	-0.092	0.189	Harvie-Moller-Weare
202	ucleus Marg	2/10/16	1.018	0.302	0.059	0.362	Harvie-Moller-Weare
202	ucleus Marg	3/11/16	0.907	-0.071	-0.176	-0.063	Harvie-Moller-Weare
198	TZ Deep	10/25/13	0.140	-1.074	-1.833	-1.246	Harvie-Moller-Weare
198	TZ Deep	11/29/13	0.260	-0.312	-0.259	-0.326	Harvie-Moller-Weare
198	TZ Deep	5/21/16	-0.606	-0.234	-0.392	-0.271	Harvie-Moller-Weare
198	TZ Deep	7/30/16	-0.369	-0.318	-0.246	-0.323	Harvie-Moller-Weare
198	TZ Deep	10/24/16	-0.330	-0.028	-0.249	-0.032	Harvie-Moller-Weare
198	TZ Deep	12/17/16	-0.544	-0.112	-0.304	-0.132	Harvie-Moller-Weare
198	TZ Deep	2/10/17	0.541	-0.105	-0.287	-0.118	Harvie-Moller-Weare
198	TZ Deep	5/24/17	-0.139	-0.014	-0.172	-0.004	Harvie-Moller-Weare
198	TZ Deep	8/21/17	-0.135	0.138	-0.066	0.171	Harvie-Moller-Weare
198	TZ Deep	11/17/17	-0.348	-0.123	-0.317	-0.143	Harvie-Moller-Weare
198	TZ Deep	11/17/17	-0.406	-0.106	-0.312	-0.125	Harvie-Moller-Weare
199	TZ Deep	11/30/13	0.106	-0.144	-0.547	-0.206	Harvie-Moller-Weare
199	TZ Deep	12/17/13	0.682	-0.090	-0.348	-0.108	Harvie-Moller-Weare
199	TZ Deep	1/14/14	-0.051	-0.116	-0.191	-0.119	Harvie-Moller-Weare
199	TZ Deep	2/19/14	0.654	-0.069	-0.126	-0.050	Harvie-Moller-Weare
199	TZ Deep	3/18/14	-0.237	-0.284	-0.268	-0.298	Harvie-Moller-Weare
199	TZ Deep	6/14/14	-0.503	-0.439	-0.871	-0.544	Harvie-Moller-Weare
199	TZ Deep	7/16/14	-0.015	-0.457	-1.136	-0.590	Harvie-Moller-Weare
199	TZ Deep	9/8/14	-0.114	-0.068	-0.246	-0.071	Harvie-Moller-Weare
199	TZ Deep	10/13/14	-0.028	-0.538	-0.184	-0.531	Harvie-Moller-Weare
199	TZ Deep	11/12/14	-0.021	-0.237	-0.670	-0.313	Harvie-Moller-Weare
199	TZ Deep	12/6/14	-0.252	-0.507	-0.928	-0.619	Harvie-Moller-Weare
199	TZ Deep	1/13/15	-0.052	-0.225	-0.664	-0.302	Harvie-Moller-Weare
199	TZ Deep	2/18/15	0.343	-0.373	-0.982	-0.491	Harvie-Moller-Weare
199	TZ Deep	3/11/15	0.399	-0.516	-0.831	-0.616	Harvie-Moller-Weare
199	TZ Deep	4/11/15	-0.095	-0.437	-1.117	-0.569	Harvie-Moller-Weare
199	TZ Deep	5/9/15	0.591	-0.488	-1.128	-0.621	Harvie-Moller-Weare
199	TZ Deep	6/10/15	-0.001	-0.313	-1.194	-0.454	Harvie-Moller-Weare
199	TZ Deep	7/14/15	0.090	-0.372	-1.134	-0.502	Harvie-Moller-Weare
199	TZ Deep	8/12/15	-0.287	-0.169	-0.689	-0.249	Harvie-Moller-Weare
199	TZ Deep	9/10/15	-0.293	-0.280	-0.465	-0.325	Harvie-Moller-Weare
199	TZ Deep	10/6/15	0.128	0.065	-0.477	0.020	Harvie-Moller-Weare
199	TZ Deep	11/10/15	0.086	-0.381	-0.473	-0.428	Harvie-Moller-Weare
199	TZ Deep	12/7/15	0.219	-0.200	-0.537	-0.258	Harvie-Moller-Weare
199	TZ Deep	1/20/16	0.139	-0.157	-0.713	-0.240	Harvie-Moller-Weare
199	TZ Deep	3/9/16	0.049	-0.151	-0.467	-0.197	Harvie-Moller-Weare
199	TZ Deep	5/21/16	-0.231	0.097	-0.296	0.085	Harvie-Moller-Weare
199	TZ Deep	10/24/16	-0.368	-0.143	-0.511	-0.195	Harvie-Moller-Weare
199	TZ Deep	12/17/16	-0.505	-0.211	-0.407	-0.253	Harvie-Moller-Weare
199	TZ Deep	2/10/17	0.916	-0.968	-2.114	-1.160	Harvie-Moller-Weare
199	TZ Deep	5/24/17	1.383	0.016	-0.419	-0.021	Harvie-Moller-Weare
199	TZ Deep	5/24/17	-0.268	-0.072	-0.359	-0.098	Harvie-Moller-Weare

199	TZ Deep	8/21/17	-0.089	-0.056	-0.354	-0.082	Harvie-Moller-Weare
199	TZ Deep	11/19/17	-0.309	-0.279	-0.829	-0.378	Harvie-Moller-Weare
200	TZ Deep	11/30/13	-0.096	-0.013	0.033	0.033	Harvie-Moller-Weare
200	TZ Deep	12/17/13	0.593	-0.163	-0.124	-0.150	Harvie-Moller-Weare
200	TZ Deep	1/14/14	-0.373	-0.143	-0.009	-0.106	Harvie-Moller-Weare
200	TZ Deep	3/18/14	-0.917	-0.609	-0.272	-0.620	Harvie-Moller-Weare
200	TZ Deep	4/19/14	-0.601	-0.300	-0.261	-0.314	Harvie-Moller-Weare
200	TZ Deep	5/14/14	-0.403	-0.084	-0.173	-0.077	Harvie-Moller-Weare
200	TZ Deep	6/15/14	-0.470	-0.178	-0.343	-0.204	Harvie-Moller-Weare
200	TZ Deep	7/21/14	-0.684	-0.086	-0.242	-0.093	Harvie-Moller-Weare
200	TZ Deep	10/13/14	-0.756	-0.071	-0.280	-0.084	Harvie-Moller-Weare
200	TZ Deep	11/12/14	-0.722	-0.290	-0.323	-0.307	Harvie-Moller-Weare
200	TZ Deep	12/5/14	-0.677	-0.082	-0.225	-0.084	Harvie-Moller-Weare
200	TZ Deep	1/14/15	-0.633	0.105	-0.286	0.094	Harvie-Moller-Weare
200	TZ Deep	2/18/15	-0.150	0.089	0.127	0.161	Harvie-Moller-Weare
200	TZ Deep	3/11/15	-0.392	-0.136	-0.280	-0.148	Harvie-Moller-Weare
200	TZ Deep	4/11/15	-0.344	0.145	-0.129	0.163	Harvie-Moller-Weare
200	TZ Deep	5/9/15	-0.288	0.041	-0.136	0.056	Harvie-Moller-Weare
200	TZ Deep	6/9/15	-0.662	0.039	-0.356	0.012	Harvie-Moller-Weare
200	TZ Deep	7/14/15	-0.294	0.076	-0.299	0.061	Harvie-Moller-Weare
200	TZ Deep	8/11/15	-0.591	0.104	-0.191	0.109	Harvie-Moller-Weare
200	TZ Deep	9/10/15	-0.611	-0.230	-0.444	-0.271	Harvie-Moller-Weare
200	TZ Deep	10/12/15	-0.576	-0.046	-0.216	-0.047	Harvie-Moller-Weare
200	TZ Deep	11/10/15	-0.384	-0.105	-0.095	-0.080	Harvie-Moller-Weare
200	TZ Deep	12/8/15	-0.132	-0.101	-0.174	-0.095	Harvie-Moller-Weare
200	TZ Deep	1/14/16	0.145	-0.416	-0.782	-0.511	Harvie-Moller-Weare
200	TZ Deep	2/16/16	-0.129	0.194	-0.088	0.221	Harvie-Moller-Weare
200	TZ Deep	3/9/16	-0.330	-0.229	-0.185	-0.225	Harvie-Moller-Weare
200	TZ Deep	5/5/16	-0.686	0.029	-0.250	0.022	Harvie-Moller-Weare
200	TZ Deep	10/23/16	-0.743	-0.011	-0.226	-0.012	Harvie-Moller-Weare
200	TZ Deep	12/17/16	-0.785	-0.114	-0.168	-0.113	Harvie-Moller-Weare
200	TZ Deep	2/11/17	-0.307	0.104	-0.096	0.128	Harvie-Moller-Weare
200	TZ Deep	5/22/17	-0.539	-0.085	-0.114	-0.067	Harvie-Moller-Weare
200	TZ Deep	8/21/17	-0.349	0.075	-0.059	0.107	Harvie-Moller-Weare
200	TZ Deep	11/19/17	-0.518	0.103	-0.294	0.087	Harvie-Moller-Weare
204	TZ Deep	10/25/13	0.245	-0.710	-0.994	-0.832	Harvie-Moller-Weare
204	TZ Deep	11/30/13	-0.089	-0.269	-0.934	-0.380	Harvie-Moller-Weare
204	TZ Deep	12/18/13	1.108	-0.221	-0.290	-0.242	Harvie-Moller-Weare
204	TZ Deep	1/17/14	0.197	-0.146	-0.302	-0.169	Harvie-Moller-Weare
204	TZ Deep	2/16/14	1.023	-0.227	-0.633	-0.304	Harvie-Moller-Weare
204	TZ Deep	5/18/14	-0.126	0.035	-0.093	0.058	Harvie-Moller-Weare
204	TZ Deep	6/12/14	0.111	0.072	-0.084	0.097	Harvie-Moller-Weare
204	TZ Deep	7/19/14	-0.199	-0.093	-0.291	-0.110	Harvie-Moller-Weare
204	TZ Deep	8/15/14	-0.074	-0.134	-0.221	-0.139	Harvie-Moller-Weare
204	TZ Deep	9/8/14	-0.011	-0.079	-0.329	-0.102	Harvie-Moller-Weare
204	TZ Deep	10/13/14	-0.178	-0.073	-0.318	-0.094	Harvie-Moller-Weare
204	TZ Deep	11/12/14	0.019	0.071	-0.356	0.044	Harvie-Moller-Weare
204	TZ Deep	12/4/14	-0.164	0.144	-0.219	0.142	Harvie-Moller-Weare
204	TZ Deep	1/12/15	-0.190	-0.008	-0.262	-0.018	Harvie-Moller-Weare
204	TZ Deep	2/16/15	0.289	0.051	-0.238	0.043	Harvie-Moller-Weare
204	TZ Deep	3/12/15	0.339	0.082	-0.220	0.081	Harvie-Moller-Weare
204	TZ Deep	6/9/15	0.085	0.072	-0.343	0.045	Harvie-Moller-Weare
204	TZ Deep	7/14/15	0.207	-0.006	-0.417	-0.047	Harvie-Moller-Weare
204	TZ Deep	8/12/15	-0.101	0.066	-0.224	0.062	Harvie-Moller-Weare
204	TZ Deep	9/9/15	-0.030	-0.212	-0.661	-0.288	Harvie-Moller-Weare
204	TZ Deep	10/7/15	0.126	0.051	-0.511	-0.005	Harvie-Moller-Weare
204	TZ Deep	11/9/15	0.244	-0.107	-0.441	-0.151	Harvie-Moller-Weare
204	TZ Deep	12/9/15	0.572	-0.070	-0.303	-0.090	Harvie-Moller-Weare
204	TZ Deep	1/13/16	0.154	-0.096	-0.175	-0.091	Harvie-Moller-Weare
204	TZ Deep	2/16/16	0.177	0.129	-0.253	0.120	Harvie-Moller-Weare
204	TZ Deep	3/10/16	0.328	-0.038	-0.310	-0.060	Harvie-Moller-Weare
205	TZ Deep	10/25/13	0.620	-0.808	-2.347	-1.007	Harvie-Moller-Weare
205	TZ Deep	11/30/13	0.215	-0.648	-1.295	-0.797	Harvie-Moller-Weare
205	TZ Deep	12/18/13	0.962	-0.518	-0.986	-0.632	Harvie-Moller-Weare
205	TZ Deep	1/16/14	0.148	-0.091	0.099	-0.035	Harvie-Moller-Weare
205	TZ Deep	2/17/14	0.885	-0.143	0.067	-0.087	Harvie-Moller-Weare
205	TZ Deep	3/23/14	0.061	0.054	-0.165	0.057	Harvie-Moller-Weare
205	TZ Deep	5/18/14	-0.042	0.072	-0.003	0.113	Harvie-Moller-Weare
205	TZ Deep	6/12/14	-0.076	-0.068	-0.150	-0.057	Harvie-Moller-Weare
205	TZ Deep	7/17/14	0.261	-0.135	-0.284	-0.152	Harvie-Moller-Weare
205	TZ Deep	8/15/14	-0.012	-0.061	-0.139	-0.049	Harvie-Moller-Weare
205	TZ Deep	11/11/14	0.102	-0.066	-0.307	-0.084	Harvie-Moller-Weare
205	TZ Deep	12/4/14	0.067	0.063	-0.167	0.071	Harvie-Moller-Weare
205	TZ Deep	1/12/15	0.371	0.141	-0.158	0.152	Harvie-Moller-Weare
205	TZ Deep	2/16/15	0.432	0.031	-0.195	0.032	Harvie-Moller-Weare
205	TZ Deep	3/11/15	0.439	0.066	-0.198	0.072	Harvie-Moller-Weare
205	TZ Deep	5/13/15	0.385	0.004	-0.153	0.013	Harvie-Moller-Weare
205	TZ Deep	6/9/15	0.049	0.000	-0.393	-0.035	Harvie-Moller-Weare
205	TZ Deep	7/14/15	0.270	-0.074	-0.484	-0.124	Harvie-Moller-Weare
205	TZ Deep	8/12/15	-0.073	0.000	-0.192	0.001	Harvie-Moller-Weare
205	TZ Deep	9/9/15	-0.016	-0.271	-0.681	-0.350	Harvie-Moller-Weare
205	TZ Deep	10/7/15	0.347	0.065	-0.382	0.031	Harvie-Moller-Weare
205	TZ Deep	11/9/15	0.469	0.340	-0.086	0.366	Harvie-Moller-Weare
205	TZ Deep	12/9/15	0.510	0.226	-0.024	0.264	Harvie-Moller-Weare
205	TZ Deep	1/13/16	0.086	-0.335	-0.594	-0.406	Harvie-Moller-Weare
205	TZ Deep	2/15/16	0.022	-0.004	-0.268	-0.016	Harvie-Moller-Weare
205	TZ Deep	3/10/16	0.387	-0.514	-0.531	-0.574	Harvie-Moller-Weare
205	TZ Deep	5/18/16	-0.168	0.040	-0.197	0.041	Harvie-Moller-Weare
205	TZ Deep	10/11/16	-0.274	0.004	-0.116	0.022	Harvie-Moller-Weare
205	TZ Deep	12/16/16	-0.420	-0.141	-0.169	-0.141	Harvie-Moller-Weare
205	TZ Deep	2/10/17	0.832	-0.222	-0.378	-0.256	Harvie-Moller-Weare
205	TZ Deep	5/22/17	0.093	-0.062	-0.081	-0.038	Harvie-Moller-Weare
205	TZ Deep	8/22/17	0.051	-0.020	0.057	0.035	Harvie-Moller-Weare
205	TZ Deep	11/18/17	-0.116	-0.249	-0.297	-0.270	Harvie-Moller-Weare
206	TZ Deep	10/25/13	0.813	-0.704	-1.747	-0.880	Harvie-Moller-Weare
206	TZ Deep	11/30/13	0.427	-0.571	-0.662	-0.651	Harvie-Moller-Weare
206	TZ Deep	12/18/13	0.908	-0.213	-0.149	-0.205	Harvie-Moller-Weare
206	TZ Deep	1/16/14	0.323	-0.145	-0.414	-0.189	Harvie-Moller-Weare
206	TZ Deep	2/17/14	0.998	-0.162	-0.571	-0.231	Harvie-Moller-Weare
206	TZ Deep	3/19/14	0.124	0.041	-0.190	0.039	Harvie-Moller-Weare
206	TZ Deep	5/18/14	0.258	0.327	-0.173	0.337	Harvie-Moller-Weare
206	TZ Deep	6/12/14	0.237	-0.060	-0.640	-0.137	Harvie-Moller-Weare
206	TZ Deep	7/17/14	0.420	-0.988	-2.948	-1.197	Harvie-Moller-Weare
206	TZ Deep	8/15/14	0.045	-0.096	-0.119	-0.079	Harvie-Moller-Weare
206	TZ Deep	10/15/14	0.146	0.074	-0.177	0.081	Harvie-Moller-Weare
206	TZ Deep	11/11/14	0.236	-0.017	-0.750	-0.108	Harvie-Moller-Weare
206	TZ Deep	1/12/15	0.273	-0.151	-1.215	-0.293	Harvie-Moller-Weare
206	TZ Deep	2/16/15	0.707	-0.079	-0.810	-0.180	Harvie-Moller-Weare
206	TZ Deep	3/11/15	0.450	-0.217	-1.227	-0.360	Harvie-Moller-Weare
206	TZ Deep	5/13/15	0.862	-0.012	-0.965	-0.130	Harvie-Moller-Weare
206	TZ Deep	6/9/15	0.279	0.000	-1.120	-0.133	Harvie-Moller-Weare
206	TZ Deep	7/15/15	0.318	-0.223	-1.281	-0.371	Harvie-Moller-Weare
206	TZ Deep	8/12/15	0.189	-0.370	-1.771	-0.549	Harvie-Moller-Weare

206	TZ Deep	9/9/15	0.161	-0.767	-1.994	-0.955	Harvie-Moller-Weare
206	TZ Deep	10/7/15	0.447	0.135	-0.670	0.055	Harvie-Moller-Weare
206	TZ Deep	11/9/15	0.236	-0.505	-0.381	-0.541	Harvie-Moller-Weare
206	TZ Deep	12/9/15	0.535	0.064	-0.076	0.091	Harvie-Moller-Weare
206	TZ Deep	1/13/16	0.339	0.039	-0.099	0.061	Harvie-Moller-Weare
206	TZ Deep	2/16/16	0.392	0.125	-0.050	0.158	Harvie-Moller-Weare
206	TZ Deep	3/9/16	0.390	0.042	-0.479	-0.008	Harvie-Moller-Weare
206	TZ Deep	5/19/16	-0.093	0.093	-0.273	0.079	Harvie-Moller-Weare
206	TZ Deep	10/10/16	-0.066	0.007	-0.625	-0.067	Harvie-Moller-Weare
206	TZ Deep	12/16/16	-0.250	0.067	-0.756	-0.028	Harvie-Moller-Weare
206	TZ Deep	2/10/17	0.585	-1.109	-2.873	-1.318	Harvie-Moller-Weare
206	TZ Deep	5/22/17	0.106	-0.164	-0.869	-0.272	Harvie-Moller-Weare
206	TZ Deep	8/22/17	0.233	-0.037	-0.592	-0.108	Harvie-Moller-Weare
206	TZ Deep	11/18/17	0.145	0.049	-0.070	0.076	Harvie-Moller-Weare
209	TZ Deep	10/24/13	0.370	-0.427	-0.206	-0.427	Harvie-Moller-Weare
209	TZ Deep	12/15/13	1.258	-0.165	-0.196	-0.150	Harvie-Moller-Weare
209	TZ Deep	1/15/14	0.743	-0.135	-0.024	-0.096	Harvie-Moller-Weare
209	TZ Deep	2/15/14	1.117	-0.123	0.003	-0.076	Harvie-Moller-Weare
209	TZ Deep	3/21/14	0.037	-0.242	-0.020	-0.204	Harvie-Moller-Weare
209	TZ Deep	4/23/14	0.430	-0.047	-0.086	-0.016	Harvie-Moller-Weare
209	TZ Deep	5/20/14	0.357	0.032	-0.006	0.080	Harvie-Moller-Weare
209	TZ Deep	6/18/14	0.372	0.035	-0.069	0.069	Harvie-Moller-Weare
209	TZ Deep	7/23/14	0.339	-0.055	-0.082	-0.026	Harvie-Moller-Weare
209	TZ Deep	10/9/14	0.349	-0.252	-0.255	-0.257	Harvie-Moller-Weare
209	TZ Deep	11/8/14	0.363	-0.123	-0.304	-0.136	Harvie-Moller-Weare
209	TZ Deep	12/6/14	0.234	-0.168	-0.225	-0.168	Harvie-Moller-Weare
209	TZ Deep	1/11/15	0.469	0.077	-0.173	0.092	Harvie-Moller-Weare
209	TZ Deep	2/16/15	0.736	-0.028	-0.217	-0.024	Harvie-Moller-Weare
209	TZ Deep	3/7/15	0.666	-0.030	-0.218	-0.026	Harvie-Moller-Weare
209	TZ Deep	4/13/15	0.517	0.083	-0.066	0.119	Harvie-Moller-Weare
209	TZ Deep	5/10/15	0.667	0.008	-0.151	0.025	Harvie-Moller-Weare
209	TZ Deep	6/4/15	0.656	-0.079	-0.052	-0.039	Harvie-Moller-Weare
209	TZ Deep	7/9/15	0.335	-0.155	-0.529	-0.210	Harvie-Moller-Weare
209	TZ Deep	8/8/15	0.375	0.116	-0.152	0.134	Harvie-Moller-Weare
209	TZ Deep	9/7/15	0.289	-0.177	-0.407	-0.208	Harvie-Moller-Weare
209	TZ Deep	10/10/15	0.774	-0.161	-0.419	-0.200	Harvie-Moller-Weare
209	TZ Deep	11/7/15	0.815	-0.116	-0.033	-0.077	Harvie-Moller-Weare
209	TZ Deep	12/6/15	0.603	-0.010	-0.071	0.023	Harvie-Moller-Weare
209	TZ Deep	1/16/16	0.852	0.070	-0.122	0.087	Harvie-Moller-Weare
209	TZ Deep	2/14/16	0.285	-0.199	-0.262	-0.207	Harvie-Moller-Weare
209	TZ Deep	5/7/16	0.214	-0.008	-0.250	-0.013	Harvie-Moller-Weare
209	TZ Deep	7/10/16	0.277	0.071	0.001	0.122	Harvie-Moller-Weare
209	TZ Deep	10/9/16	0.074	0.032	-0.153	0.053	Harvie-Moller-Weare
209	TZ Deep	12/20/16	0.211	0.003	-0.019	0.045	Harvie-Moller-Weare
209	TZ Deep	2/9/17	1.031	-0.067	-0.150	-0.051	Harvie-Moller-Weare
209	TZ Deep	5/23/17	0.191	-0.061	-0.407	-0.090	Harvie-Moller-Weare
209	TZ Deep	5/23/17	0.831	0.076	0.162	0.163	Harvie-Moller-Weare
209	TZ Deep	8/24/17	0.804	0.401	-0.027	0.444	Harvie-Moller-Weare
209	TZ Deep	11/15/17	0.414	-0.020	-0.285	-0.031	Harvie-Moller-Weare
210	TZ Deep	10/24/13	0.436	-0.415	-0.082	-0.399	Harvie-Moller-Weare
210	TZ Deep	11/29/13	0.998	-0.052	-0.018	-0.017	Harvie-Moller-Weare
210	TZ Deep	12/14/13	1.762	-0.065	-0.193	-0.066	Harvie-Moller-Weare
210	TZ Deep	1/15/14	1.212	0.168	-0.321	0.145	Harvie-Moller-Weare
210	TZ Deep	2/15/14	1.532	-0.032	-0.143	-0.020	Harvie-Moller-Weare
210	TZ Deep	4/23/14	0.823	0.011	-0.235	0.008	Harvie-Moller-Weare
210	TZ Deep	5/20/14	0.487	-0.061	-0.225	-0.065	Harvie-Moller-Weare
210	TZ Deep	6/18/14	0.743	0.106	-0.093	0.131	Harvie-Moller-Weare
210	TZ Deep	7/23/14	0.562	-0.038	-0.335	-0.062	Harvie-Moller-Weare
210	TZ Deep	10/9/14	0.695	-0.240	-0.335	-0.264	Harvie-Moller-Weare
210	TZ Deep	11/8/14	0.705	-0.097	-0.351	-0.124	Harvie-Moller-Weare
210	TZ Deep	1/11/15	0.846	0.212	-0.169	0.222	Harvie-Moller-Weare
210	TZ Deep	2/16/15	1.018	-0.019	-0.277	-0.033	Harvie-Moller-Weare
210	TZ Deep	3/7/15	0.876	-0.029	-0.179	-0.023	Harvie-Moller-Weare
210	TZ Deep	4/14/15	0.874	0.092	-0.223	0.090	Harvie-Moller-Weare
210	TZ Deep	5/10/15	0.898	0.023	-0.294	0.007	Harvie-Moller-Weare
210	TZ Deep	6/4/15	1.020	0.112	-0.183	0.118	Harvie-Moller-Weare
210	TZ Deep	7/9/15	0.654	-0.137	-0.638	-0.212	Harvie-Moller-Weare
210	TZ Deep	8/8/15	0.586	0.049	-0.289	0.033	Harvie-Moller-Weare
210	TZ Deep	9/7/15	0.364	-0.352	-0.543	-0.412	Harvie-Moller-Weare
210	TZ Deep	10/10/15	0.514	-0.150	-0.539	-0.210	Harvie-Moller-Weare
210	TZ Deep	11/7/15	1.588	0.078	-0.383	0.047	Harvie-Moller-Weare
210	TZ Deep	12/6/15	0.782	0.039	-0.182	0.044	Harvie-Moller-Weare
210	TZ Deep	1/16/16	0.896	0.060	-0.379	0.029	Harvie-Moller-Weare
210	TZ Deep	2/14/16	0.866	0.163	-0.143	0.177	Harvie-Moller-Weare
210	TZ Deep	5/7/16	0.533	0.069	-0.340	0.046	Harvie-Moller-Weare
210	TZ Deep	7/10/16	0.526	0.086	-0.257	0.078	Harvie-Moller-Weare
210	TZ Deep	10/9/16	0.417	0.130	-0.209	0.131	Harvie-Moller-Weare
210	TZ Deep	12/19/16	0.265	-0.159	-0.203	-0.165	Harvie-Moller-Weare
210	TZ Deep	2/9/17	1.240	-0.070	-0.238	-0.076	Harvie-Moller-Weare
210	TZ Deep	5/23/17	0.599	0.063	-0.059	0.093	Harvie-Moller-Weare
210	TZ Deep	8/24/17	0.780	0.104	-0.223	0.102	Harvie-Moller-Weare
210	TZ Deep	11/15/17	0.484	-0.220	-0.552	-0.282	Harvie-Moller-Weare
150	TZ Margin	2/12/13	1.391	-0.097	-0.245	-0.114	Harvie-Moller-Weare
150	TZ Margin	5/22/13	1.263	-0.084	0.095	-0.028	Harvie-Moller-Weare
150	TZ Margin	6/11/13	1.294	-0.073	-0.189	-0.078	Harvie-Moller-Weare
150	TZ Margin	8/18/13	1.478	-0.138	-0.130	-0.131	Harvie-Moller-Weare
150	TZ Margin	9/5/13	1.284	-0.064	0.123	-0.003	Harvie-Moller-Weare
150	TZ Margin	10/17/13	1.496	-0.092	0.010	-0.057	Harvie-Moller-Weare
214	TZ Margin	10/17/13	0.903	-0.050	-0.153	-0.041	Harvie-Moller-Weare
214	TZ Margin	11/27/13	1.058	-0.046	-0.004	-0.010	Harvie-Moller-Weare
214	TZ Margin	12/11/13	1.548	-0.257	-0.062	-0.219	Harvie-Moller-Weare
214	TZ Margin	1/17/14	1.008	0.078	0.044	0.132	Harvie-Moller-Weare
214	TZ Margin	2/12/14	0.472	-0.086	-0.138	-0.070	Harvie-Moller-Weare
214	TZ Margin	4/17/14	0.838	0.004	-0.149	0.013	Harvie-Moller-Weare
214	TZ Margin	6/12/14	0.864	0.010	0.037	0.054	Harvie-Moller-Weare
214	TZ Margin	8/17/14	0.775	0.035	-0.081	0.060	Harvie-Moller-Weare
214	TZ Margin	10/8/14	0.808	-0.480	-0.183	-0.475	Harvie-Moller-Weare
214	TZ Margin	11/7/14	0.828	-0.061	-0.228	-0.064	Harvie-Moller-Weare
214	TZ Margin	12/5/14	0.170	-0.558	-1.455	-0.717	Harvie-Moller-Weare
214	TZ Margin	1/7/15	0.858	0.030	0.107	0.097	Harvie-Moller-Weare
214	TZ Margin	2/12/15	1.082	-0.045	-0.206	-0.044	Harvie-Moller-Weare
214	TZ Margin	3/3/15	1.037	0.002	-0.070	0.031	Harvie-Moller-Weare
214	TZ Margin	4/11/15	0.723	-0.042	-0.291	-0.055	Harvie-Moller-Weare
214	TZ Margin	5/6/15	0.825	0.028	-0.129	0.046	Harvie-Moller-Weare
214	TZ Margin	6/7/15	0.646	-0.165	-0.357	-0.192	Harvie-Moller-Weare
214	TZ Margin	7/12/15	0.994	0.147	-0.255	0.139	Harvie-Moller-Weare
214	TZ Margin	8/6/15	0.710	-0.139	-0.231	-0.144	Harvie-Moller-Weare
214	TZ Margin	9/3/15	0.489	-0.223	-0.449	-0.266	Harvie-Moller-Weare
214	TZ Margin	10/11/15	0.772	-0.056	-0.104	-0.033	Harvie-Moller-Weare
214	TZ Margin	11/11/15	0.949	-0.105	-0.015	-0.066	Harvie-Moller-Weare
214	TZ Margin	12/5/15	1.072	0.081	0.033	0.128	Harvie-Moller-Weare
214	TZ Margin	1/18/16	0.854	0.018	-0.195	0.017	Harvie-Moller-Weare
214	TZ Margin	2/10/16	0.989	0.115	-0.012	0.156	Harvie-Moller-Weare

214	TZ Margin	3/11/16	0.944	0.081	-0.071	0.107	Harvie-Moller-Weare
245	TZ Margin	10/24/13	1.155	-0.181	-1.870	-0.364	Harvie-Moller-Weare